DOI: 10.26599/FSHW.2025.9250809

Contents lists available at SciOpen

Food Science and Human Wellness

journal homepage: https://www.sciopen.com/journal/2097-0765

China Food Publishing Co.

Metabolomic and Intestinal-microbial Profiling to Interpret the Mitigation of Water-soluble and insoluble Polysaccharides and Triterpenoids from *Poria cocos* against Glucolipid Metabolic Disorders

Cheng-Zhu Song [a,b,#], Hui-Qiong Yang [a,b,#], Wei-Mei Yu [a,b], Zhong-Yu Fu [a,b], Yu-Xuan Tao [a,b], Mei Zhang [a,b], Yan Qi [a,b], Jie Yu [a,b,*], Xing-Xin Yang [a,b,*]

[a] *College of Pharmaceutical Science, Yunnan University of Chinese Medicine, 1076 Yuhua Road, Kunming 650500, China*

[b] *Yunnan Key Laboratory of Southern Medicine Utilization, 1076 Yuhua Road, Kunming 650500, China*

ABSTRACT: The chemical components of *Poria cocos* (PC) mainly include water-soluble polysaccharides (WSP), water-insoluble polysaccharides (WIP), and triterpenoids (TP). PC treats glucolipid metabolic disorders (GLMD), but studies on the effects and mechanisms of WSP, WIP, and TP on GLMD are lacking. GLMD rat model induced by high-fat and high-sugar diet (HFHSD) was used to evaluate the effects of TP, WSP, and WIP on GLMD. TP, WSP, and WIP were collected from PC, with purities of 88%, 90%, and 91%, respectively. They decreased lipid levels in serum and liver, reduced hepatic steatosis and blood sugar, improved insulin resistance, as well as gastrointestinal and liver mitochondrial function. Differential metabolites involved in the regulation of metabolic pathways were restored to the normal values by TP, WSP, and WIP. TP and WIP regulated EPT1, LCAT, and LPCAT2 levels in the glycerophospholipid metabolism pathway, while WSP regulated EPT1 and LCAT levels in the glycerophospholipid metabolism pathway. TP and WIP regulated sPLA2 level in the arachidonic acid metabolism pathway. TP, WSP, and WIP regulated ALDH7A1 level in the lysine degradation pathway. TP, WSP, and WIP regulated the diversity, richness, and community structure of gut microbiome at the phylum, genus, and species levels associated with the pharmacological indicators total cholesterol (TC), triglyceride (TG), and acetyl choline (ACH), as well as several metabolic pathways. Therefore, TP, WSP, and WIP alleviated GLMD by ameliorating gastrointestinal and liver mitochondrial function, mainly involved in the regulation of lipid, amino acid, cofactors, and vitamins, and gut microbiome. They constitute the main material basis for PC's efficacy against GLMD.

Keywords: Glucolipid metabolism; Gut microbiome; Metabolomics; Polysaccharides; *Poria cocos*; Triterpenes

1. Introduction

Glucose and lipid metabolism is a vital life process for the body's energy and material supply. Glucolipid metabolic disorders (GLMD) are a group of metabolic diseases characterized by abnormal blood glucose levels, dyslipidemia, and insulin resistance. These disorders are closely associated with the development and progression of chronic diseases such as diabetes, obesity, and cardiovascular diseases[1-4]. Its pathogenesis involved neuroendocrine disorder, insulin resistance, oxidative stress, interinflammatory disease and

# These authors contributed equally to this work
***Corresponding author**
yxx78945@163.com; cz.yujie@gmail.com

Received 16 February 2025
Received in revised from 13 March 2025
Accepted 24 April 2025

intestinal flora disorder[4]. Long-term high-fat and high-sugar diet (HFHSD) and sedentary lifestyle further aggravate the GLMD[5, 6]. Commonly, lifestyle intervention is the main therapeutic approach to prevent and/or treat GLMD. At present, no specific remedies have been reported to treat GLMD. Therefore, it is of great value to find effective remedies in the prevention and treatment of GLMD.

Poria cocos (PC) is a fungus commonly used in traditional Chinese medicine with a long history of medicinal use[7]. It is commonly used in the treatment of edema, gastrointestinal dysfunction, and diarrhea, as well as symptoms such as restlessness, palpitations, and insomnia[8, 9]. Modern pharmacological studies showed that PC has many pharmacological actions, including diuresis, liver protection, anti-tumor, anti-fatty liver, hypolipidemic, anti-inflammation, anti-virus, anti-oxidation, and anti-aging effects, as well as blood sugar, gut microbiota properties, and gastrointestinal regulation[10-13]. Therefore, PC holds promising potential for development as a therapeutic agent against GMLD.

The chemical components of PC mainly include water-soluble polysaccharides (WSP), water-insoluble polysaccharides (WIP), and triterpenoids (TP), representing 90% of PC[12]. Crude polysaccharides[14], WIP[15] and triterpenoids[16-18] (such as pachymic acid, polyporenic acid C, and eburicoic acid) derived from PC have demonstrated promising effects in regulating blood sugar or lipids. The ethanol extract of PC regulates mitochondrial function and bile acid metabolism to alleviate metabolic dysfunction-associated fatty liver disease[19, 20]. However, the effects and mechanisms of WSP, WIP and TP on GLMD are unclear. Particularly, the comparison of efficacy and mechanisms of these three components on GLMD are still lacking.

Metabonomics can reveal the specific changes of physiological and biochemical states related to phenotypes in biological systems[21]. It has thus emerged as a powerful tool in metabolic disease research, offering unique capabilities in early disease detection, mechanistic elucidation, precision therapeutics, treatment monitoring, and pharmaceutical development[22-25]. The human intestine harbours highly complex and diverse microorganisms that possess essential functions in host physiology[26]. Intestinal dysbacteriosis is linked with many diseases including GLMD, obesity, type 2 diabetes, hepatic steatosis, intestinal bowel diseases and several types of cancer[27]. This study employed a HFHSD-induced GLMD rat model to evaluate the pharmacological effects of three components of PC on GLMD. Then, an integrated multi-omics approach combining UHPLC/MS metabolomics and 16S rRNA microbiome analysis was used to explore the therapeutic mechanisms of three components against GLMD. The results indicated that TP, WSP, and WIP alleviated HFHSD-induced GLMD by ameliorating gastrointestinal and liver mitochondrial function, which mainly involved the regulation of the metabolism of lipid, amino acid, cofactors, and vitamins, as well as gut microbiome.

2. Material and Methods

2.1. Chemicals and materials

Metformin (MF) was purchased from Abbott Laboratories (Abbott Park, IL, USA). The basic basal rodent diet and HFHSD were purchased from SYSE Bio-tech Co., Ltd. (Kunming, China). Standard D-galactose (Gal), D-mannose (Man), D-glucose (Glu), L-arabinose (Ara), L-fucose (Fuc), L-rhamnose

(Rha), D-galacturonic acid (GalA), and D-glucuronic acid (GlcA) were purchased from RENI Pharmaceutical Technology Co., Ltd. (Chengdu, China) with a purity greater than 98%. Commercial kits for the determination of triglyceride (TG), total cholesterol (TC), alanine transaminase (ALT), aspartate transaminase (AST), low-density lipoprotein cholesterol (LDL-C), high-density lipoprotein cholesterol (HDL-C), ATP synthase (ATPase), acetyl choline (ACH), D-xylose, malondialdehyde (MDA), and glutathione (GSH) activity were purchased from Nanjing Jiancheng Bioengineering Institute (Nanjing, China). Kits for determining mitochondrial respiratory chain complex I and II (MRCC I and II), motilin (MTL), gastrin (GAS), interleukin-1 β (IL-1β), interleukin-2 (IL-2), interleukin-6 (IL-6), insulin (INS), lecithin cholesterol acyltransferase (LCAT), lysophosphatidylcholine acylacyltransferase 2 (LPCAT2), secretory phospholipase A2 (sPLA2), and aldehyde dehydrogenase family 7 member A1 (ALDH7A1) were obtained from Jiangsu Meimian Industrial Co., Ltd. (Jiangsu, China). The kit for determining ethanolamine phosphonate transferase 1 (EPT1) was obtained from Jianglai Biotech Co. (Shanghai, China). Hematoxylin and eosin (HE) stain kit was purchased from Solarbio Co., Ltd. (Shanghai, China). Oil red O dye was purchased from Sigma-Aldrich (St. Louis, MO, USA). HPLC-grade methanol and acetonitrile were purchased from Merck (Darmstadt, Germany). PF Mag-Bind Stool DNA Kit was purchased from Omega Bio-tek (Georgia, U.S.). FastPfu Polymerase was purchased from TransGen Biotech Co., Ltd. (Beijing, China). Deionized water was purified by a Milli-Q Water Purification System (Millipore, Billerica, MA, USA). All the reagents were of analytical reagent grade or higher. The PC samples were purchased from Medicinal Herb Market in Pu'er City (China) and authenticated by Professor Jie Yu at the Yunnan University of Chinese Medicine. The PC voucher specimen was deposited in the Key Laboratory of Southern Medicine Utilization, Yunnan University of Chinese Medicine (Kunming, China). TP, WSP, and WIP were successfully harvested from PC, achieving purities of 88%, 90%, and 91% (Table S1), respectively, and their specific chemical compositions were characterized. The methods of preparation and chemical characterization of TP, WSP, and WIP are presented in the Supplementary Material.

2.2. Animal experiment

2.2.1. Animals and design

Healthy male Sprague Dawley rats (200 ± 50) g were purchased from SPF (Beijing) Biotechnology Co., Ltd. (Beijing, China). The rats were housed in a standard environment ((22 ± 1) ℃ temperature, 60% ± 10% humidity, and a 12 h/12 h light/dark cycle) with free access to water and food. Experiments were performed according to the Guide for the Care and Use of Laboratory Animals as prepared by the National Academy of Sciences and published by the National Institutes of Health. The animal protocol was reviewed and approved by the Institutional Ethical Committee on Animal Care and Experimentations of Yunnan University of Chinese Medicine (Ethics number R-062022144).

After one week of adaptive feeding, rats were randomly divided into twelve groups (six rats per group): control group (CON; normal saline), model group (MOD; normal saline), MF group (90 mg/kg), low-dose TP group (LTP; 75 mg/kg), medium-dose TP group (MTP; 150 mg/kg), high-dose TP group (HTP; 300 mg/kg),

low-dose WSP group (LWSP; 75 mg/kg), medium-dose WSP group (MWSP; 150 mg/kg); high-dose WSP group (HWSP; 300 mg/kg), low-dose WIP group (LWIP; 75 mg/kg), medium-dose WSP group (MWIP; 150 mg/kg), and high-dose WSP group (HWIP; 300 mg/kg). The doses of 75, 150, and 300 mg/kg were selected for this study were based on previous applications of WSP in high-fat diet-induced atherosclerosis research[27]. To enable a direct comparison of the pharmacological effects and mechanisms of action among WSP, WIP, and TP, WIP and TP were administered at the same dosage levels. MF, TP, WSP, and WIP were separately prepared in normal saline. All rats in each group were treated with a dose of 1 mL/100 g by intragastric administration once a day for 10 weeks. All groups except the CON group were fed HFHSD (composed of 72% basic diet, 10.9% lard, 15% sucrose, 2% cholesterol, 0.1% pig bile salt) for 10 weeks to establish the rat GLMD model. The amount of diet was recorded every day during the experiment and the weight was recorded once a week.

2.2.2. Sample collection

After HFHSD feeding for 8 weeks, rats were fasted for 12 h and treated with an intragastric administration of 3% D-xylose (1 mL/100 g). The urine samples were collected in a metabolic cage for the next 5 hours and stored at -80 ℃ for the measurement of the D-xylose level. At week 10, urine samples were collected in a metabolic cage for the next 24 hours and stored at -80 ℃ for metabolome analysis. At the end of the 10-week experiment, all rats were fasted for 12 h and anesthetized (10% sodium pentobarbital injected intraperitoneally at a dose of 0.3–0.4 mL/100 g). Blood was taken from the abdominal aorta and allowed to clot at 4 ℃. Subsequently, serum samples were obtained by centrifuging the blood at 3,500 r/min for 15 min and stored at -80 ℃. The liver, stomach, small intestine and cecal content were collected. A portion of the liver tissue was fixed in 4% paraformaldehyde and electron microscope fixation solution for HE staining, oil red O staining, and transmission electron microscopy (TEM). The stomach and small intestine were fixed in 4% paraformaldehyde for HE staining. All the other samples were flash-frozen in liquid nitrogen and stored at -80 ℃.

2.2.3. Detection of glycolipid-related indexes

After blood was collected from the tail vein, the level of FBG was assessed using a blood glucose test strip and blood glucose monitoring meter system (Sinocare, Changsha, China) at week 4, 8 and 10. The level of INS in the serum was determined using commercially available assay kits at week 10, and the data were obtained using a SpectraMax Plus 384 Microplate Reader (Molecular Devices, Sunnyvale, CA, USA). The HOMA-IR [INS (mU/L) * FBG (mmol/L)/22.5] was then calculated. All rats were fasted for 12 h before the tests.

The histopathological changes in the liver were evaluated by HE staining. Liver samples were collected from the same location, fixed and dehydrated in a 4% formaldehyde solution, embedded in paraffin and cut into 4 μm-thick sections using a paraffin-embedding machine and microtome (Leica, Wetzlar, Germany). The sections were routinely stained with HE, and sealed with neutral gum. Additionally, lipid accumulation in the liver was assessed by oil red O staining. The liver sample was collected and embedded in optimal cutting

temperature compound, and frozen at -20 ℃ for 30 min. The liver sample was then cut into 8 μm-thick sections and fixed to a glass slide, which was then immersed in 60% isopropyl alcohol for 5 s. The slides were stained with oil red O solution (containing 60% isopropyl alcohol) for 15 minutes, washed repeatedly with phosphate buffered saline, stained with hematoxylin for 10 s, and sealed with glycerin gelatin. Finally, images of oil red O and HE staining were captured using a CX31 Olympus imaging system (Olympus Corporation, Tokyo, Japan).

The levels of ALT, AST, TG, TC, LDL-C, and HDL-C in the serum were measured using a biochemical analyzer (Beckman CX4, Roche, Germany). Additionally, their levels in the supernatant from liver homogenate were determined using commercially available assay kits, according to the manufacturer's instructions. The data were obtained using a SpectraMax Plus 384 Microplate Reader (Molecular Devices, Sunnyvale, CA, USA).

2.2.4. Detection of gastrointestinal function

After HFHSD feeding for 10 weeks, the stomach and small intestine were fixed and dehydrated in a 4% paraformaldehyde solution, embedded in paraffin, cut, and stained with HE to evaluate the histological changes. Images were captured using a CX31 Olympus imaging system (Olympus Corporation, Tokyo, Japan).

The levels of IL-1β, IL-6, IL-2 ACH, GAS, and MTL in the serum and D-xylose in the urine were measured using commercially available assay kits, following the manufacturer's protocol. The data were obtained using a SpectraMax Plus 384 Microplate Reader (Molecular Devices, Sunnyvale, CA, USA).

2.2.5. Measurement of mitochondrial function in the liver

TEM was used to investigate the changes of the mitochondria ultrastructure. The liver was fixed in 0.01% phosphate buffer (pH 7.4 with 2.5% glutaraldehyde) and then in 0.24 M phosphate buffer (pH 7.4 with 1% osmium tetroxide). Next, the sample was rinsed in phosphate buffered saline, dehydrated in ethanol and acetone gradients (20%, 30%, 50%, 70%, 90% and 100%), embedded in Epon resin, cut into thin slices, stained with uranyl acetate and lead citrate in turn. Finally, images were captured using a HT7700 transmission electron microscope (HITACHI, Tokyo, Japan).

Liver mitochondria were isolated as previously described and resuspended in saline[28]. The levels of MDA, GSH, Ca^{2+}-Mg^{2+}-ATPase, Na^{+}-K^{+}-ATPase, MRCC I and II in the mitochondrial suspension were measured using commercially available assay kits according to the manufacturer's instructions. The data were obtained using a SpectraMax Plus 384 Microplate Reader (Molecular Devices, Sunnyvale, CA, USA).

2.2.6. Metabolome analysis

Metabolites were extracted from the liver, serum and urine, detected by ultra-high performance liquid chromatography/mass spectrometry, and identified using HMDB, Metlin, and a self-built database of Majorbio. Statistical analyses were applied to confirm significantly-altered metabolites (VIP $>$ 1, $P <$

0.05). Pathway analysis was performed using KEGG, and enrichment was assessed via Fisher's exact test. The detailed analytical procedures are described in the Supplementary Material.

2.2.7. Evaluation of sPLA2, ALDH7A1, LCAT, LPCAT2, and EPT1 expression in the liver

Metabolic pathway diagrams were developed for glycerophospholipid and arachidonic acid metabolism as well as lysine degradation using the KEGG database (https://www.kegg.jp/) to identify key enzymes involved in these metabolic pathways. The expression of the key enzymes in the supernatant of the liver samples, such as sPLA2, ALDH7A1, LCAT, LPCAT2, and EPT1, were measured using commercially available assay kits, according to the manufacturer's instructions. The data were obtained using a SpectraMax Plus 384 Microplate Reader (Molecular Devices, Sunnyvale, CA, USA).

2.2.8. 16S rRNA gene sequencing and analysis

The bacterial genomic DNA in the caecum content of rats was extracted using commercially available assay kits, according to the manufacturer's instructions. 16S rRNA gene sequencing was determined by the Illumina PE300 platform (Illumina, San Diego, CA, USA). Data analysis of alpha diversity, beta diversity, and species composition and difference were performed on the Majorbio Cloud platform (https://cloud.majorbio.com). The detailed methods are provided in the Supplementary Material.

2.2.9. Correlation analysis

The correlation analysis of intestinal flora, metabolic pathways, differential metabolites, and pharmacodynamic indicators was performed on the Majorbio Cloud platform (https://cloud.majorbio.com). The network was constructed using Cytoscape 3.8.2 (https://cytoscape.org/).

2.2.10. Statistical analysis

Statistical analysis was performed using GraphPad Prism 8.3.5 (GraphPad Software, CA, USA). Differences among multiple groups were analyzed with one-way ANOVA followed by Dunnett's test or Kruskal-Wallis sum test followed by Tukey-Kramer post hoc test. Results were expressed as mean ± standard deviation (S.D.). A value of $P < 0.05$ was considered statistically significant.

3. Results

3.1. Chemical characterization of WSP, WIP, and TP

WSP and WIP did not show any evident absorption peaks in UV-Vis spectra at 260 and 280 nm, indicating that WSP and WIP contains low levels of proteins and nucleic acids (Fig. S1A). WSP contained 0.3726% polyphenols, 0.2651% proteins, and 7.1933% ash, while WIP showed significantly lower levels at 0.0510% polyphenols, 0.0016% proteins, and 6.7834% ash, confirming their high purity (Table S1).

The retention time of WSP was 9.173 min, and the molecular weight (Mw) and the number-average molecular weight (Mn) were 36.696 kDa and 30.255 kDa, respectively (Table S2 and Fig. S1B). The polydispersity index (polydispersity index: Mw/Mn) was 1.21. These results suggested that WSP was a relatively homogeneous polysaccharide. The retention time of WIP was 6.566 min, and Mw and Mn were

421.875 kDa and 136.591 kDa, respectively, with polydispersity index of 3.08, indicating that the molecular weight distribution of WIP was wide.

WSP consisted of Glu, Fuc, Man and Gal in a monosaccharide ratio of 12.84%, 17.87%, 25.67%, and 43.62%, respectively (Fig. S1C). WIP consisted of Glu and glucuronic acid in a monosaccharide ratio of 90.67% and 9.33%, respectively.

The fourier transform spectra of WSP and WIP are shown in Fig. S1D. As regards WSP, the strong and broad peak was approximately at 3423.41 cm^{-1}, which was due to the O-H stretch vibration. The adsorption around 2918.38 cm^{-1} was due to the C-H stretching vibration bond of CH3 or CH2. The sharp peak at 1632.63cm^{-1} suggested the existence of a stretching vibration of a free carboxylate group. The strong adsorption peak at 1074.99 cm^{-1} was due to the stretching vibration of the pyranose ring. As regards WIP, the strong adsorption peak was approximately at 3431.83 cm^{-1} and it was due to the O-H stretch vibration. The adsorption peak observed around 2924.69 cm^{-1} was due to the C-H stretching vibration bond of CH3 or CH2. The absorption peak around 1066.57 cm^{-1} was the resonance absorption peak of the pyranose ring and hydroxy-O-H, and the absorption peak around 883.49 cm^{-1} was the characteristic absorption peak of β-glycoside bond.

SEM observation revealed that WSP was mainly spine-like, with a compact structure and a network distribution, while WIP exhibited an irregular spherical shape with some pores and loose structure (Fig. S1E).

A total of 60 triterpenoid molecules were identified in TP, including dehydropachymic acid, pachymic acid, polyporenic acid C, and tumulosic acid (Table S3).

3.2. Effects of TP, WSP, and WIP on physiological and biochemical parameters in GLMD rats

3.2.1. Effects of TP, WSP, and WIP on glycolipids in GLMD rats

The body weight of rats in all groups increased after 10 weeks of HFHSD feeding, and no significant difference was observed in the body weight and food intake of rats among all groups, indicating that TP, WSP, and WIP did not significantly affect the normal food intake and body weight of rats (Fig. S2).

The level of INS in the serum significantly increased after HFHSD feeding, with an upward trend of FBG level; the value of HOMA-IR also increased significantly, indicating a significant insulin resistance (Table 1 and Fig. 1A). The levels of FBG, INS and the value of HOMA-IR significantly decreased after the administration of TP, WSP, and WIP, suggesting that they prevented FBG increase and insulin resistance induced by HFHSD. The liver of rats after 10 weeks of HFHSD feeding was swollen with degeneration of hepatocytes, hepatic steatosis, ballooning, and lipid droplet deposition (Fig. 1B-C). HFHSD-induced liver histopathology was improved after the administration of TP, WSP, and WIP, and lipid droplet deposition was decreased. The levels of TC, TG, LDL-C, ALT, and AST in the serum and liver after 10 weeks of HFHSD feeding were significantly increased, while the level of HDL-C was significantly decreased (Fig. 1D-E). These effects were reversed after the treatment with TP, WSP, and WIP, indicating that they regulated the serum and liver lipid metabolism disorders caused by HFHSD.

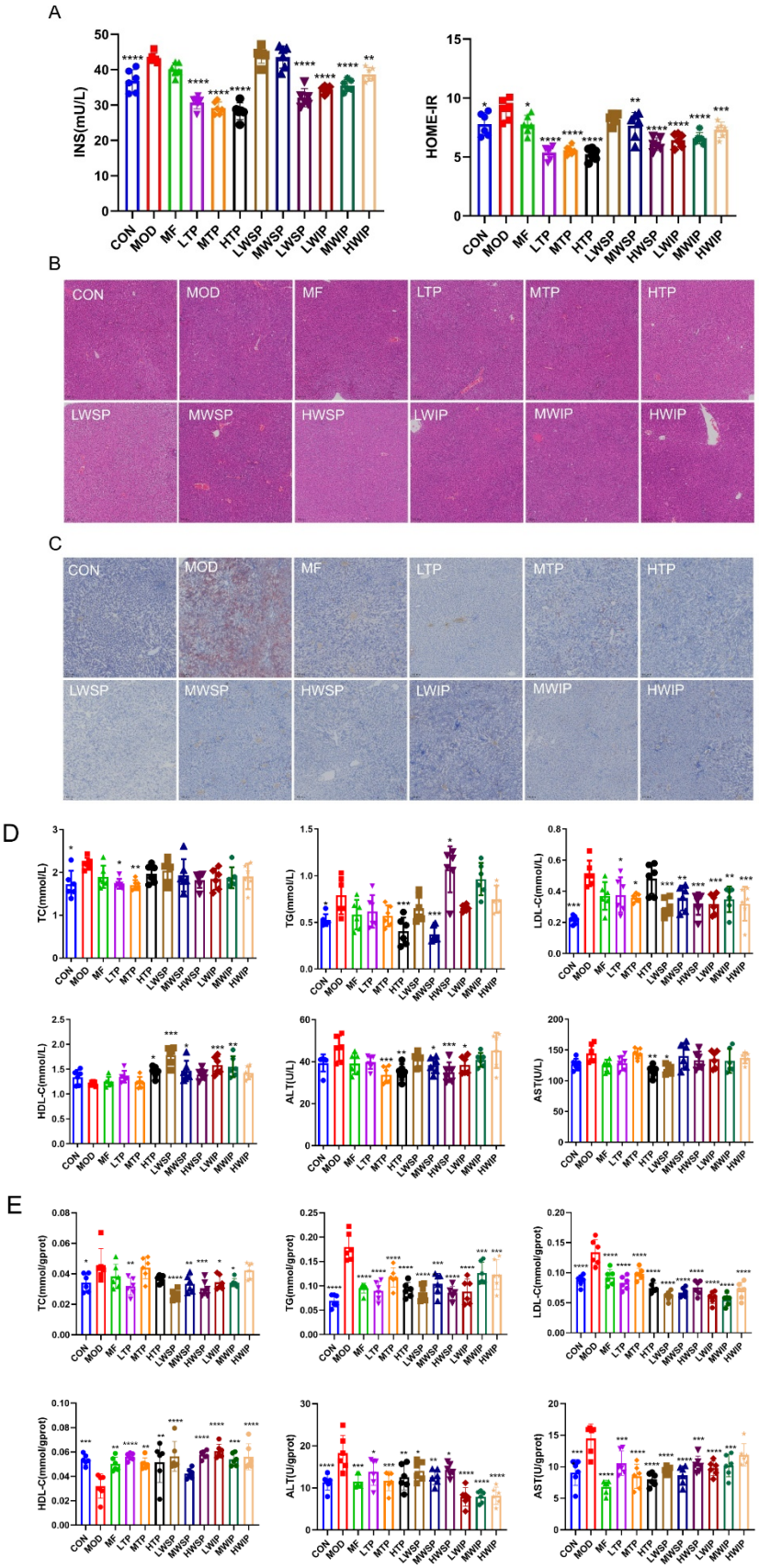

FIGURE 1. Effects of TP, WSP, and WIP on glycolipids in GLMD rats. Sprague Dawley rats were treated with saline, MF (90 mg/kg/day), TP, WSP, or WIP (75, 150, or 300 mg/kg/day). Rats were sacrificed after 10 weeks of HFHSD feeding and the serum and liver were collected. The level of FBG was assessed using blood glucose test strip and blood glucose monitoring meter system. The level of INS in the serum was determined and the HOMA-IR [INS (mU/L) * FBG (mmol/L)/22.5] was calculated (A). Liver histology after HE (B) and oil red O staining (C) observed under light microscopy (10x magnification, scale bar = 100 μm). Levels of TC, TG, ALT, HDL-C, LDL-C and AST in both serum (D) and liver (E) measured. Results are expressed as mean ± S.D. from 6 animals. *$P < 0.05$, **$P < 0.01$, ***$P < 0.001$, ****$P < 0.0001$ *vs.* MOD group.

3.2.2. Effects of TP, WSP, and WIP on the gastroenteric function in GLMD rats

A large number of necrotic epithelial cells were present in the gastric tissues after 10 weeks of HFHSD feeding, and the gastric pits architecture formed by gastric mucosal epithelial cells disappeared (Fig. 2A). The administration of TP, WSP, and WIP resulted in the disappearance of a small number of necrotic epithelial cells of the gastric mucosa, as well as the gastric pits in the local gastric mucosa, with no evident pathological changes. The overall structure of the small intestinal tissue, as well as that of the crypt-villuswas abnormal after 10 weeks of HFHSD feeding (Fig. 2B). The structure of some villi was incomplete, and the mucosal epithelial cells were detached. The structure of the small intestinal tissue was restored to normal after the administration of TP, WSP, and WIP. The structure of small intestinal villi and mucosal epithelium was intact, and no substantial epithelial cells sloughing was observed. The serum levels of IL-1β and IL-6 showed an increasing trend, whereas the level of IL-2 showed a decreasing trend after 10 weeks of HFHSD feeding (Fig. 2C). These effects were reversed by the treatment with TP, WSP, and WIP, indicating that they alleviated gastrointestinal inflammation in GLMD rats. The levels of GAS, MTL, and ACH in the serum and D-xylose in the urine significantly decreased after 10 weeks of HFHSD feeding (Fig. 2D). However, the levels of ACH, MTL in the serum significantly increased after the administration of TP. The level of ACH in the serum significantly increased after the administration of WSP, and the levels of MTL, GAS and D-xylose in the urine showed an increasing trend. The levels of ACH, MTL, and GAS in the serum significantly increased after the administration of WIP, and the level of D-xylose in the urine showed an increasing trend. These results suggested that TP, WSP, and WIP promoted stomach and intestinal movement, protected gastrointestinal mucosa and improved gastrointestinal function.

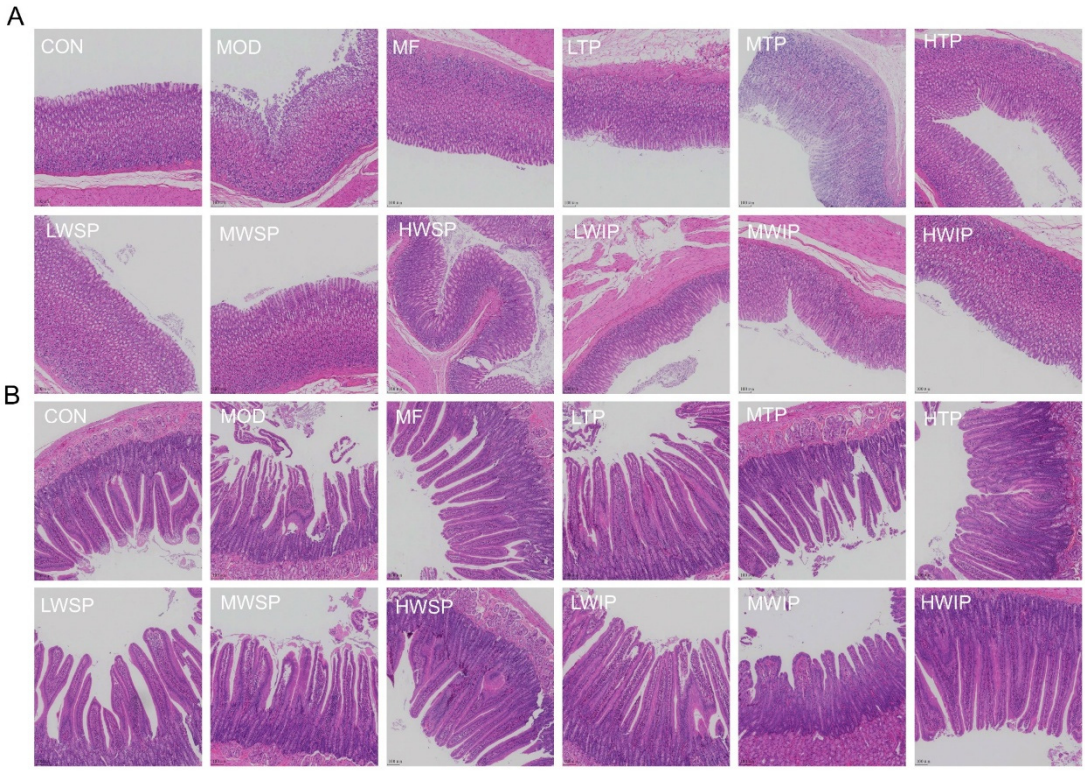

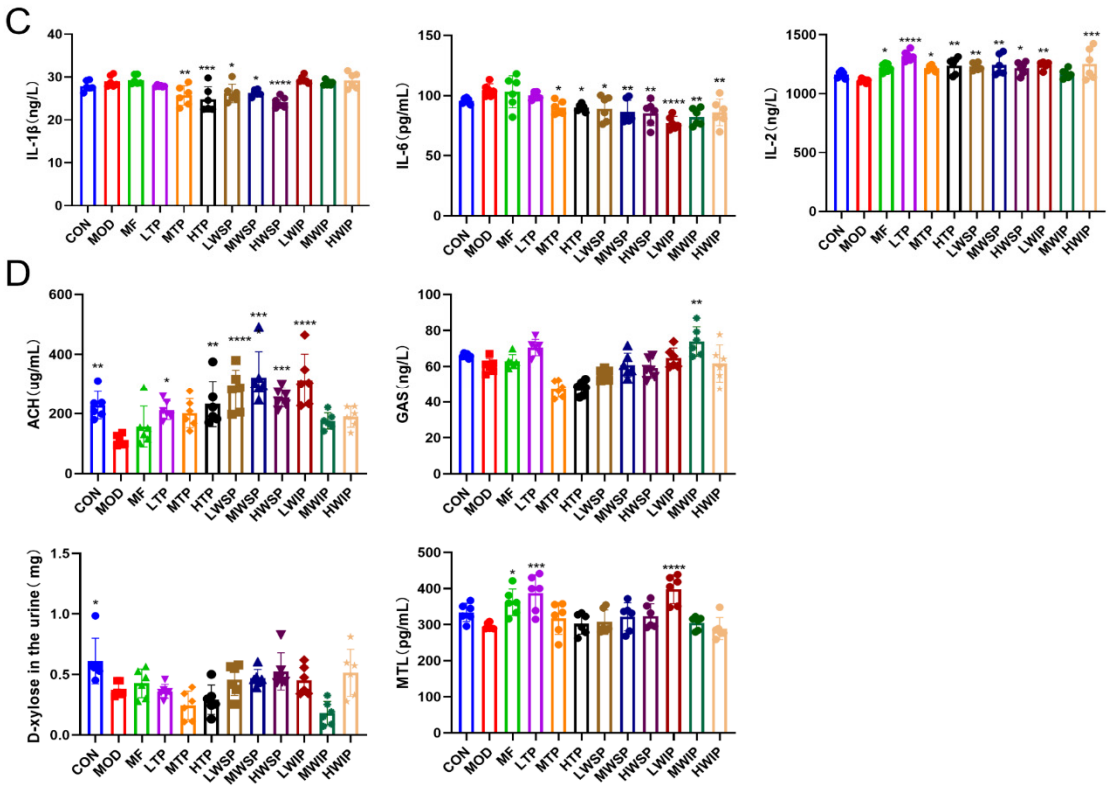

FIGURE 2. Effects of TP, WSP, and WIP on the gastroenteric function in GLMD rats.

Sprague Dawley rats were treated with saline, MF (90 mg/kg/day), TP, WSP, or WIP (75, 150, or 300 mg/kg/day). Rats were sacrificed after 10 weeks of HFHSD feeding, and serum, stomach and small intestine were collected. Histology of the stomach (A) and small intestine (B) after HE staining observed under light microscopy (10x magnification, scale bar = 100 μm). Levels of IL-1β, IL-6, and IL-2 in the serum measured using commercially available assay kits (C). Levels of ACH, GAS, and MTL in the serum and levels of D-xylose in the urine measured using commercially available assay kits (D). Results are expressed as mean ± S.D. from 6 animals. *$P < 0.05$, **$P < 0.01$, ***$P < 0.001$, ****$P < 0.0001$ *vs*. MOD group.

3.2.3. Effects of TP, WSP, and WIP on mitochondrial function in the liver in GLMD rats

The ultrastructure of liver mitochondria showed evident swelling and rupture after 10 weeks of HFHSD feeding (Fig. 3A). The mitochondrial volume increased, the outer membrane was partially blurred and broken (Fig. 3A I, indicated by the arrow), the intramembranous matrix was locally dissolved and lightened (Fig. 3A II, indicated by the arrow), and the cristae were heavily fractured and reduced (Fig. 3A III, indicated by the arrow). These damages were attenuated after the administration of TP. The levels of Ca^{2+}-Mg^{2+}-ATPase and MRCC I in liver mitochondria were significantly reduced after 10 weeks of HFHSD feeding, the levels of GSH, MRCC II and Na^{+}-K^{+}-ATPase in liver mitochondria showed a downward trend, while the level of MDA was significantly increased (Fig. 3B). However, the levels of MRCC II and Ca^{2+}-Mg^{2+}-ATPase in liver mitochondria significantly increased after the administration of TP, the levels of GSH, MRCC I, and Na^{+}-K^{+}-ATPase showed an increasing trend, while the levels of MDA showed a decreasing trend. However, the levels of GSH, MRCC I, MRCC II, Na^{+}-K^{+}-ATPase, and Ca^{2+}-Mg^{2+}-ATPase in the liver mitochondria significantly increased after the administration of WSP, while the level of MDA showed a decreasing trend. The level of MRCC II in the liver mitochondria significantly increased after the administration of WIP, the levels of GSH, MRCC I, Na^{+}-K^{+}-ATPase, and Ca^{2+}-Mg^{2+}-ATPase showed an increasing trend, while the level of MDA showed a decreasing trend.

These results demonstrated that TP, WSP, and WIP protected mitochondrial function, reduced oxidative stress damage, and improved energy metabolism, consequently ameliorating HFHSD-induced GLMD.

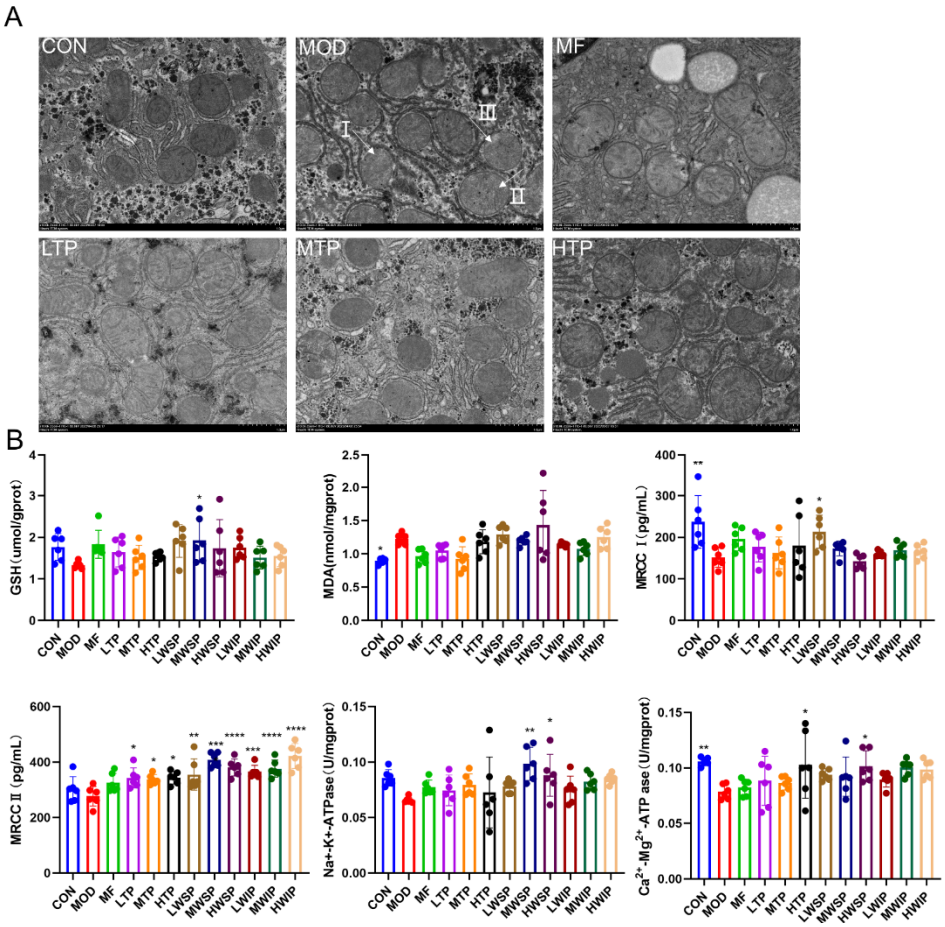

FIGURE 3. Effects of TP, WSP, and WIP on mitochondrial function in GLMD rats.

Sprague Dawley rats were treated with saline, MF (90 mg/kg/day), TP, WSP, or WIP (75, 150, or 300 mg/kg/day). Rats were sacrificed after 10 weeks of HFHSD feeding, the liver was collected, and liver mitochondria were isolated. Liver mitochondrial ultrastructure was assessed by TEM (A). Levels of MDA, GSH, Ca^{2+}-Mg^{2+}-ATPase, Na^{+}-K^{+}-ATPase, MRCC I and II in the mitochondrial suspension measured using commercially available assay kits (B). Results are expressed as mean ± S.D. from 6 animals. *$P < 0.05$, **$P < 0.01$, ***$P < 0.001$, ****$P < 0.0001$ *vs*. MOD group.

3.3. Effects of TP, WSP, and WIP on metabolites in the serum, urine, and liver of GLMD rats

The PCA and PLS-DA plots showed that the clustering of each group was well distinguished in both electrospray ionization (ESI^{+} and ESI^{-}) modes, and metabolites of the three main component groups tended to the normal group, suggesting that TP, WSP, and WIP induced evident metabolic changes in GLMD rats (Fig. 4A-B). OPLS-DA analysis demonstrated a significant difference in the overall abundance of metabolites in the urine, serum, and liver of the TP, WSP, and WIP groups, compared to that in the MOD group (Fig. S3). A total of 588 (Table S4-6), 500 (Table S7-9), and 308 (Table S10-12) differential metabolites were identified in the serum, urine, and liver samples after TP, WSP, and WIP administration, respectively.

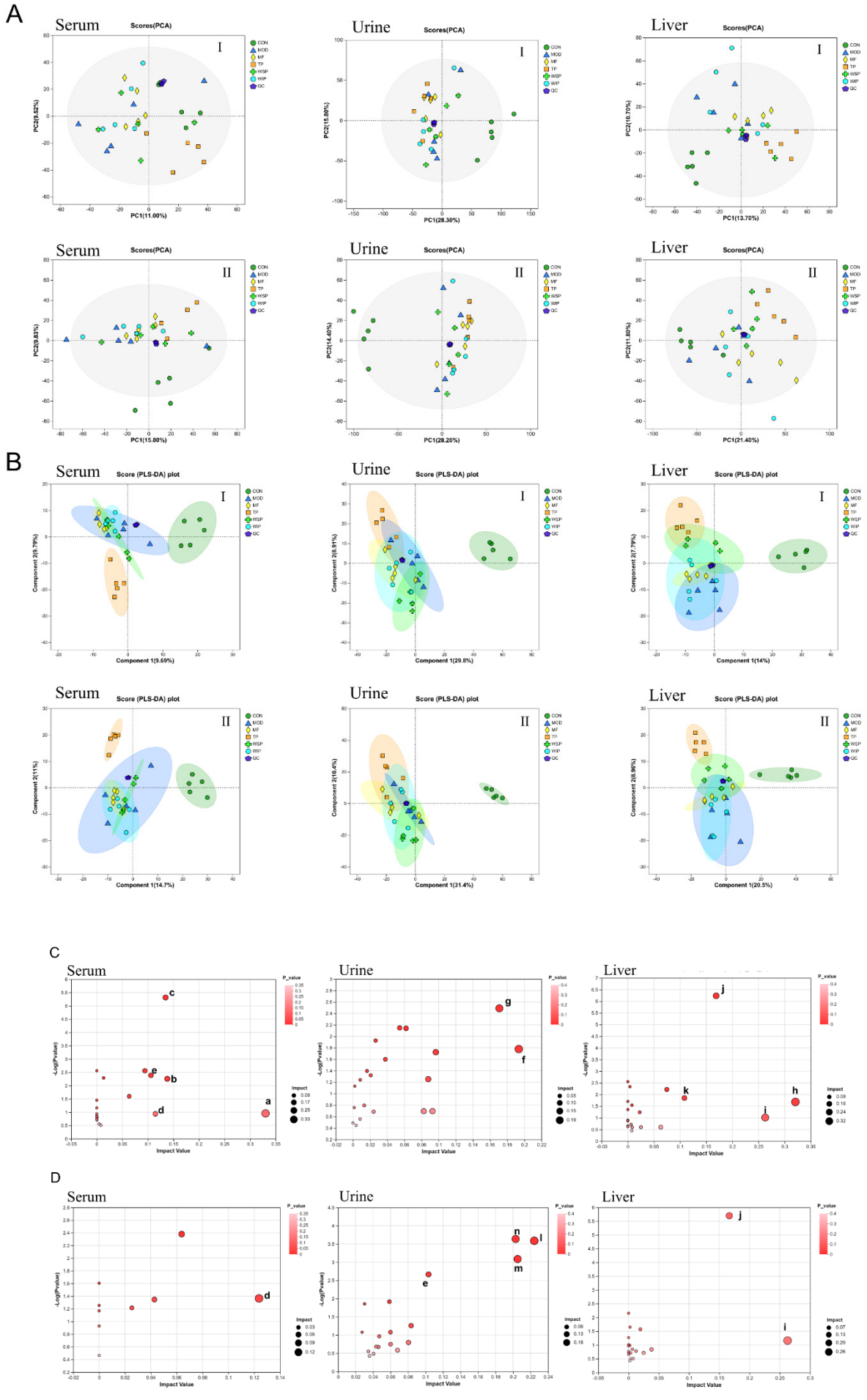
A
Serum
Scores(PCA)
I
PC1(11.00%)
PC2(9.62%)
Urine
Scores(PCA)
I
PC1(28.30%)
PC2(15.80%)
Liver
Scores(PCA)
I
PC1(13.70%)
PC2(10.70%)
Serum
Scores(PCA)
II
PC1(15.80%)
PC2(9.83%)
Urine
Scores(PCA)
II
PC1(28.20%)
PC2(14.40%)
Liver
Scores(PCA)
II
PC1(21.40%)
PC2(11.80%)
CON
MOD
MF
TP
WSP
WIP
QC
B
Serum
Score (PLS-DA) plot
I
Component 1(9.69%)
Component 2(9.79%)
Urine
Score (PLS-DA) plot
I
Component 1(29.8%)
Component 2(8.91%)
Liver
Score (PLS-DA) plot
I
Component 1(14%)
Component 2(7.79%)
Serum
Score (PLS-DA) plot
II
Component 1(14.7%)
Component 2(11%)
Urine
Score (PLS-DA) plot
II
Component 1(31.4%)
Component 2(10.4%)
Liver
Score (PLS-DA) plot
II
Component 1(20.5%)
Component 2(8.96%)
C
Serum
Urine
Liver
-Log(Pvalue)
Impact Value
P_value
Impact
a
b
c
d
e
f
g
h
i
j
k
D
Serum
Urine
Liver
-Log(Pvalue)
Impact Value
P_value
Impact
d
e
i
j
l
m
n

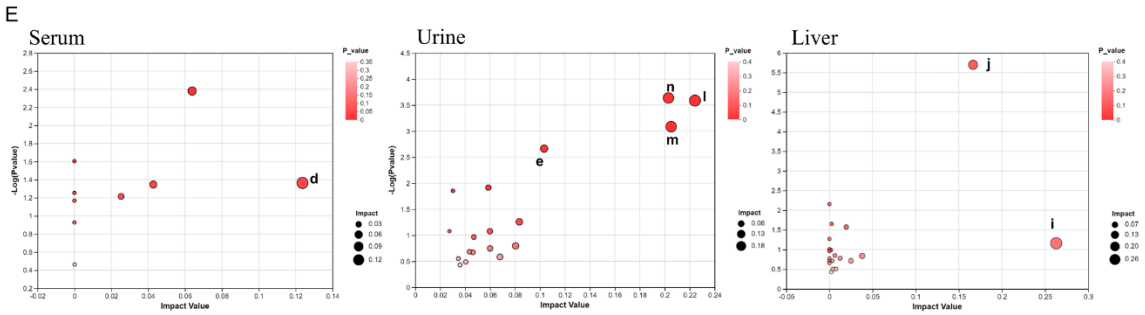

FIGURE 4. Effects of TP, WSP, and WIP on metabolites in serum, urine, and liver in GLMD rats. Sprague Dawley rats were treated with saline, MF (90 mg/kg/day), TP, WSP, or WIP (75, 150, or 300 mg/kg/day). Rats were sacrificed after 10 weeks of HFHSD feeding, and serum, urine, and liver were collected for metabolomics analysis (n = 5 per group). PCA (A) and plot PLS-DA (B) of the serum, urine and liver samples in both positive (I) and negative (II) ion modes. Differential metabolic pathways (a-o; shown in Table 4-6) regulated by TP (D), WSP (E), and WIP (F).

Pathway enrichment analysis on the differentially classified metabolites revealed that the differential metabolites in the serum, urine, and liver samples of TP-treated rats were involved in 11 metabolic pathways such as glycerophospholipid, arachidonic acid, taurine, hypotaurine, arginine, proline, glycine, serine, threonine, sphingolipid, tyrosine, alanine, aspartate, glutamate, retinol, and α-linolenic acid metabolism and polycyclic aromatic hydrocarbon degradation. The differential metabolites in the serum, urine, and liver samples of WSP-treated rat shown in Fig. 4D and Table 3 were involved in 7 metabolic pathways such as glycerophospholipid, sphingolipid, histidine, tyrosine, and retinol metabolism, lysine degradation, and lysine biosynthesis (Table 2). The differential metabolites in the serum, urine, and liver samples of WIP-treated rats shown in Fig. 4E and Table 4 were involved in 3 metabolic pathways, including the metabolism of glycerophospholipids, glycine, serine, and threonine, as well as the biosynthesis of benzoxazines. These results suggested that TP, WSP, and WIP improved GLMD by regulating metabolic pathways.

Table 2. Differential metabolic pathways regulated by TP.

NO.	Pathway description	Match_status	Impact_value
a	Taurine and hypotaurine metabolism	1|22	0.330151
b	Arginine and proline metabolism	3|67	0.137898
c	Glycine, serine and threonine metabolism	5|47	0.134594
d	Sphingolipid metabolism	1|23	0.114754
e	Tyrosine metabolism	3|60	0.106048
f	Alanine, aspartate and glutamate metabolism	2|28	0.193478
g	Polycyclic aromatic hydrocarbon degradation	3|42	0.170804
h	Arachidonic acid metabolism	2|37	0.320593
i	Retinol metabolism	1|17	0.262887
j	Glycerophospholipid metabolism	6|52	0.16899
k	alpha-Linolenic acid metabolism	2|30	0.108247

Table 3. Differential metabolic pathways regulated by WSP.

NO.	Pathway description	Match_status	Impact_value
d	Sphingolipid metabolism	1|23	0.123696
l	Lysine biosynthesis	4|34	0.224230
m	Lysine degradation	4|46	0.205177
n	Histidine metabolism	4|33	0.202984
e	Tyrosine metabolism	4|60	0.103392
i	Retinol metabolism	1|17	0.262887
j	Glycerophospholipid metabolism	5|52	0.166578

Table 4. Differential metabolic pathways regulated by WIP.

NO	Pathway Desciption	Match_status	Impact_value
c	Glycine, serine and threonine metabolism	3|47	0.134174
o	Benzoxazinoid biosynthesis	1|9	0.142857
j	Glycerophospholipid metabolism	2|52	0.111783

3.4. Effects of TP, WSP, and WIP on sPLA2, ALDH7A1, LCAT, LPCAT2, and EPT1 levels in the liver of GLMD rats

Lecithin, dimethylethanolamine, phosphatidylethanolamine, phosphatidylserine, and phosphatidylglycerol in the glycerophospholipid metabolism pathway were increased, whereas 1-acyl-sn-glycero-3-phosphocholine were decreased after TP treatment (Fig. S4A). Moreover, lecithin, phosphatidylethanolamine, phosphatidylserine, and phosphatidylglycerol were increased, while 1-acyl-sn-glycero-3-phosphocholine and phosphatidyl-L-serine were decreased after WSP treatments(Fig. S4B). Similarly, phosphatidylethanolamine was increased, whereas and 1-acyl-sn-glycero-3-phosphocholine and lecithin were decreased after WIP treatments(Fig. S4C). Lecithin was increased whereas arachidonate was decreased in the arachidonic acid metabolism pathway after TP treatment (Fig. S5A). L-lysine and L-2-aminoadipat in the lysine degradation pathway were increased, whereas 2-oxoadipate and 2-oxoglutarate were decreased after WSP treatments (Fig. S6A). The variations of these metabolites might be attributed to the regulation of key enzymes (such as LCAT, LPCAT2, EPT1, sPLA2, and ALDH7A1) by TP, WSP, and WIP. The interactions between these enzymes and metabolites are shown in Fig. S4D, Fig. S5B and Fig. S6B.

Consequently, the expression of key enzymes involved in the regulation of metabolites in glycerophospholipid and arachidonic acid metabolism, as well as lysine degradation were further investigated. The expression of LPCAT2 in the liver after 10 weeks of HFHSD feeding was significantly reduced, while the expression of EPT1 and LCAT showed a downward trend, indicating that HFHSD feeding disrupted the glycerophospholipid metabolic pathway (Fig. 5A-C). However, the expression of LCAT and LPCAT2 significantly increased, and the expression of EPT1 showed an downward trend after the treatment with TP. The expression of EPT1 significantly increased and LCAT showed an up-ward trend, whereas the expression of LPCAT2 did not significantly changed after the treatment with WSP. The expression of EPT1 significantly increased, and the expression of LCAT and LPCAT2 showed an upward trend after the treatment with WIP. These results indicated that TP, WSP, and WIP effectively regulated the expression of key regulatory enzymes, reversed the disorder of glycerophospholipid metabolism, adjusted the metabolite contents, consequently improving GLMD.

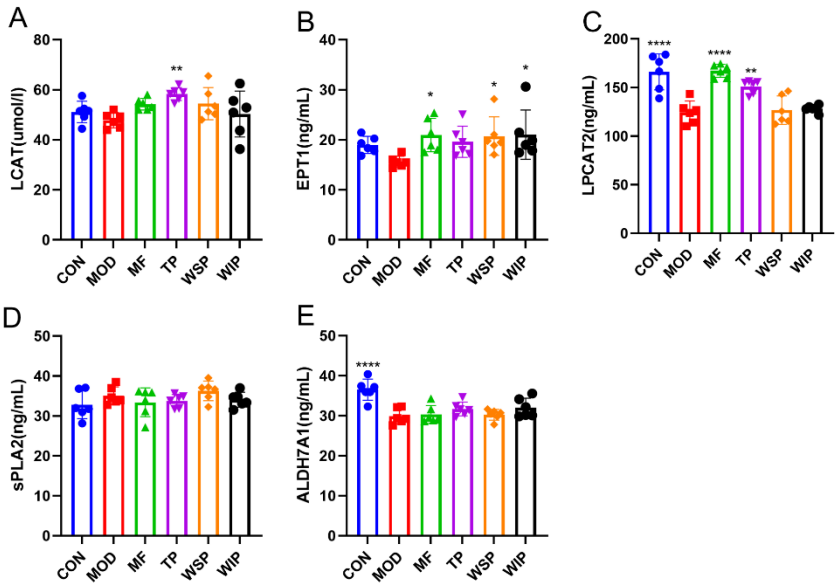

FIGURE 5. Effects of TP, WSP, and WIP on sPLA2, ALDH7A1, LCAT, LPCAT2, and EPT1 levels in the liver of GLMD rats. Sprague Dawley rats were treated with saline, MF (90 mg/kg/day), TP, WSP, or WIP (75, 150, or 300 mg/kg/day). Rats were sacrificed after 10 weeks of HFHSD feeding and the liver was collected. Levels of LCAT (A), EPT1(B), LPCAT2 (C), sPLA2 (D) and ALDH7A1 (E) measured using commercially available assay kits. Results are expressed as mean ± S.D. from 6 animals. *$P < 0.05$, **$P < 0.01$, ***$P < 0.001$ *vs*. MOD group.

The expression of sPLA2 in the liver showed an up-ward trend after 10 weeks of HFHSD feeding (Fig. 5D). However, the expression of sPLA2 showed a downward trend after the treatment with TP. In contrast, WSP treatment resulted in an upward trend of sPLA2, while WIP treatment resulted in its downward trend. These findings indicated that both TP and WIP inhibited lecithin decomposition by activating the arachidonic acid metabolism pathway, thereby reducing arachidonate synthesis and improving GLMD.

The expression of ALDH7A1 in the liver was significantly down-regulated after 10 weeks of HFHSD feeding (Fig. 5E). However, its expression showed an up-regulated trend after the treatment with TP, WSP, and WIP, indicating that they activated the lysine degradation pathway to improve GLMD.

3.5. Effects of TP, WSP, and WIP on gut microbiotas in GLMD rats

The effect of TP, WSP, and WIP on the α-diversity of gut microbial community was evaluated using the Chao, Ace, Sobs, Shannon, and Simpson indices; the first four significantly decreased after 10 weeks of HFHSD feeding, while the Simpson index showed an increasing trend, suggesting that HFHSD reduced the diversity and richness of gut microbiota in the GLMD rats (Fig. 6). However, these changes were reversed by the treatment of TP, WSP, and WIP, indicating that they increased the richness and diversity of intestinal microbiota.

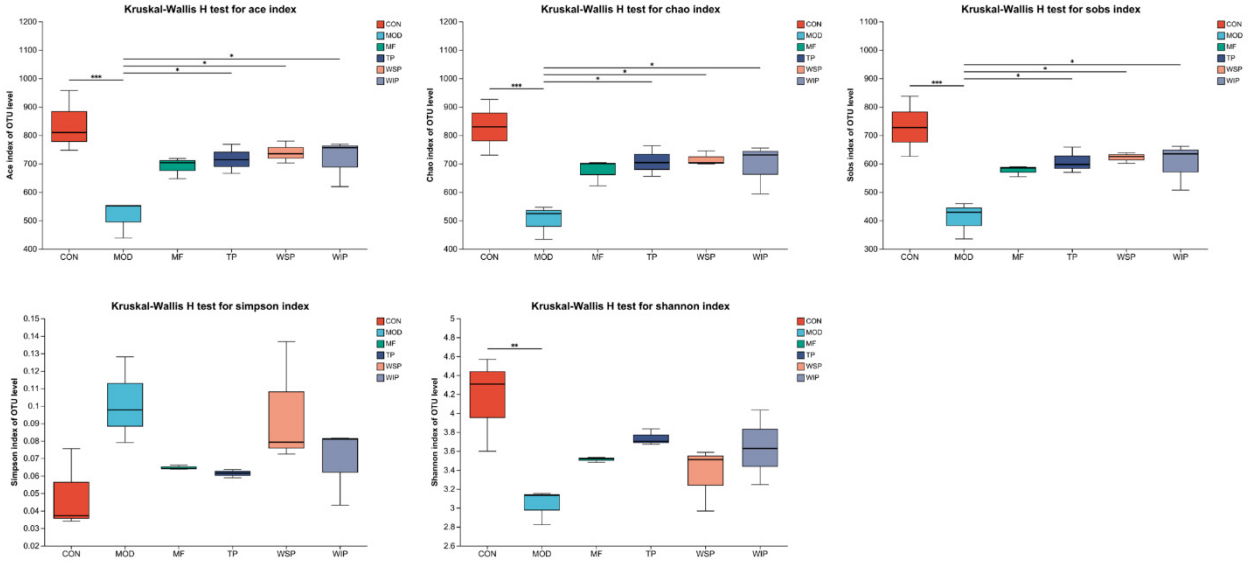

FIGURE 6. Effects of TP, WSP, and WIP on the diversity and richness of gut microbiotas in GLMD rats. Sprague Dawley rats were treated with saline, MF (90 mg/kg/day), TP, WSP, or WIP (75, 150, or 300 mg/kg/day). The cecum was collected after 10 weeks of HFHSD feeding for 16S rRNA sequencing analysis. α-diversity of the gut microbial community evaluated by the Ace (A), Chao (B), Sobs (C), Shannon (D), and Simpson (E) indices. Results are expressed as mean ± S.D. from 3 animals. *$P < 0.05$, **$P < 0.01$, **$P < 0.001$ *vs*. MOD group.

β-diversity analysis was performed to measure the differences in gut microbial communities among different groups. NMDS, PCA, and PCoA analysis were performed on gut microbiota of each group at the OUT level, which revealed a separation among the six experimental groups (Fig. 7A-C). The MOD and CON group were distributed in different quadrants, and the significant differences between the administration groups and MOD group were observed. Furthermore, the administration groups were closer to the CON group compared with the MOD group. This result indicated the structural change in gut microbiome due to HFHSD feeding, and the treatment with TP, WSP, and WIP restored the composition of the gut microbial community to normal.

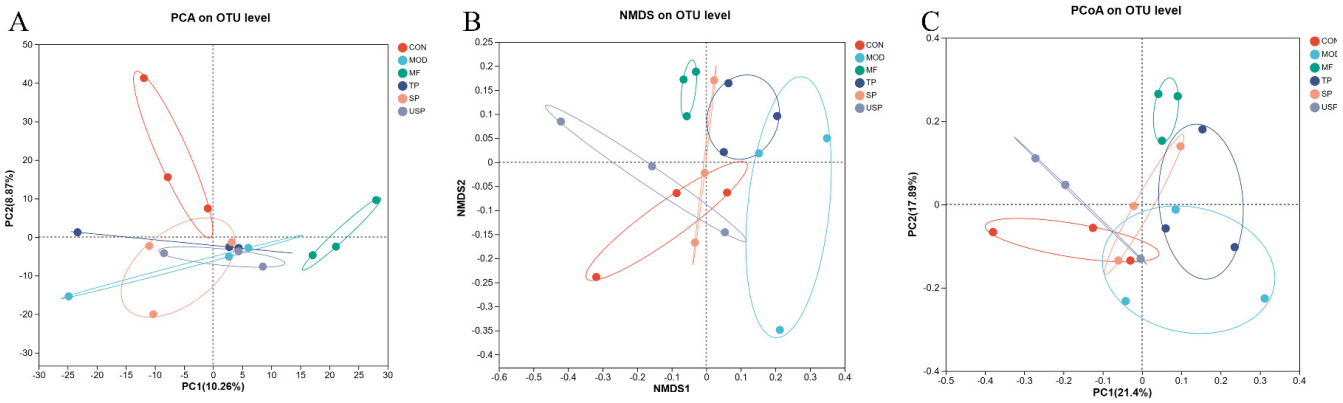

FIGURE 7. Effects of TP, WSP, and WIP on the structure of gut microbiotas in GLMD rat. Sprague Dawley rats were treated with saline, MF (90 mg/kg/day), TP, WSP, or WIP (75, 150, or 300 mg/kg/day). The cecum was collected after 10 weeks of HFHSD feeding for 16S rRNA sequencing analysis. β-diversity analysis was performed to measure the differences in gut microbial communities among all the groups. PCA (A), NMDS (B), and PCoA (C) analysis showing β-diversity among six groups at the OUT level ($n = 3$ per group).

Fig. 8A shows the top ten most abundant phylum in the intestine of the rats treated with TP, WSP, and WIP, such as Firmicutes, Actinobacteriota, Patescibacteria, Bacteroidota, Spirochaetota, Desulfobacterota,

Cyanobacteria, Proteobacteria, unclassified_k__norank_d__Bacteria, and Campilobacterota. The gut microbiota of each group was dominated by Firmicutes and Actinobacteriota at the phylum level. The relative abundance of Actinobacteriota significantly increased, while Spirochaetota and Bacteroidota significantly decreased after 10 weeks of HFHSD feeding (Fig. 8B-D). However, the relative abundance of Actinobacteriota significantly decreased, while that of Spirochaetota and Bacteroidota significantly increased after WSP treatment. The relative abundance of *Actinobacteriota*in significantly decreased, while that of Spirochaetota and Bacteroidota did not obvious change after WIP treatment. However, no significant change was observed in the relative abundance of Actinobacteriota, Spirochaetota and Bacteroidota after TP treatment. These results showed that WSP alleviated GLMD through the regulation of Actinobacteriota, Spirochaetota and Bacteroidota, WIP alleviated GLMD through the regulation of Actinobacteriota, while TP did not have any significant regulatory effect on these gut microbiotas.

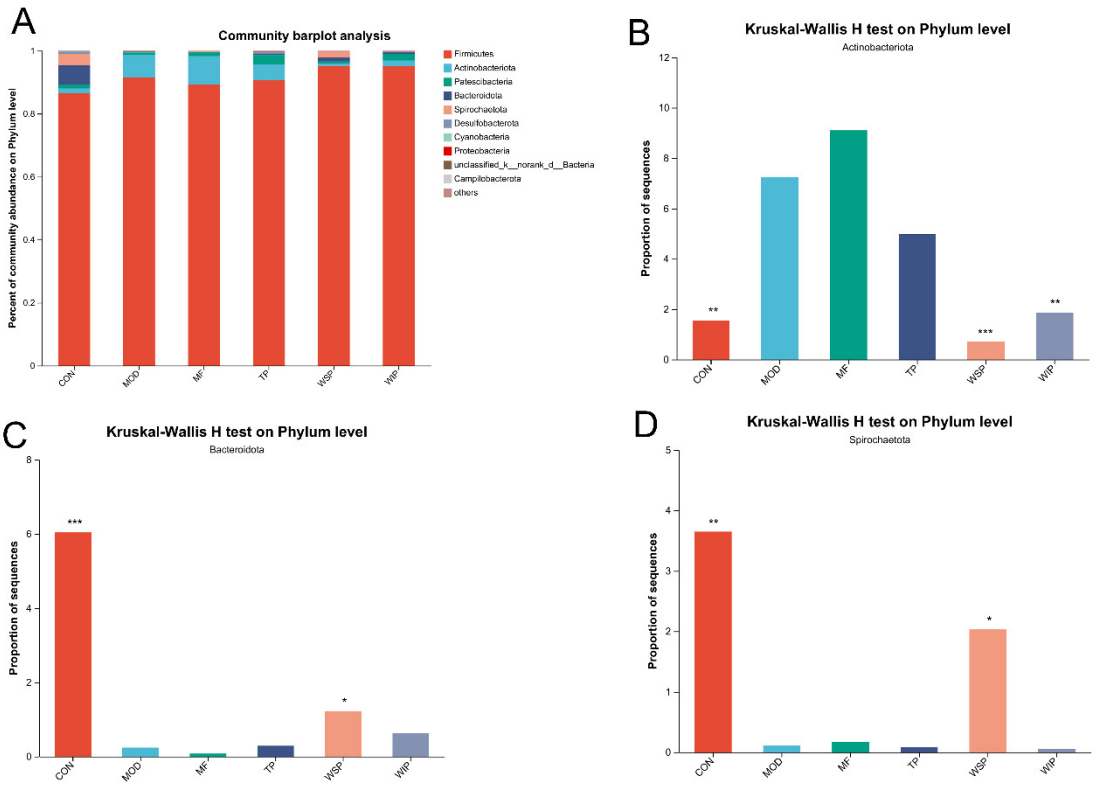

FIGURE 8. Effects of TP, WSP, and WIP on species composition and species difference of gut microbiotas in GLMD rats at the phylum level. Sprague Dawley rats were treated with saline, MF (90 mg/kg/day), TP, WSP, or WIP (75, 150, or 300 mg/kg/day). The cecum content was collected after 10 weeks of HFHSD feeding for 16S rRNA sequencing analysis. Effect of TP, WSP, and WIP on species composition at the phylum level (A). Effects of TP, WSP, and WIP on species difference of gut microbiota at the phylum level in (B-D). Results are expressed as mean ± S.D. from 3 animals. **P* < 0.05, ***P* < 0.01, ****P* < 0.001 *vs*. MOD group.

Fig. 9A shows the top ten most abundant genus in the intestine of the rats treated with TP, WSP, and WIP, such as *Lactobacillus*, *Romboutsia*, *Faecalibaculum*, *Clostridium_sensu_stricto_1*, *Blautia*, *norank_f__norank_o__Clostridia_UCG-014*, *Turicibacter*, *Allobaculum*, *Bifidobacterium*, and *UCG-005*. The relative abundance of *Clostridium_sensu_stricto_1*, *Allobaculum*, and *Bifidobacterium* significantly increased after 10 weeks of HFHSD feeding (Fig. 9B-D). However, the relative abundance of *Clostridium_sensu_stricto_1*, *Allobaculum* and *Bifidobacterium* significantly decreased after WSP treatment.

The relative abundance of *Bifidobacterium* significantly decreased after WIP treatment. However, these significant changes were not observed after TP treatment. These results revealed that WSP alleviated GLMD through the regulation of *Clostridium_sensu_stricto_1*, *Allobaculum* and *Bifidobacterium*, and WIP alleviated GLMD through the regulation of *Bifidobacterium*, while TP did not have any significant regulatory effect on these gut microbiotas.

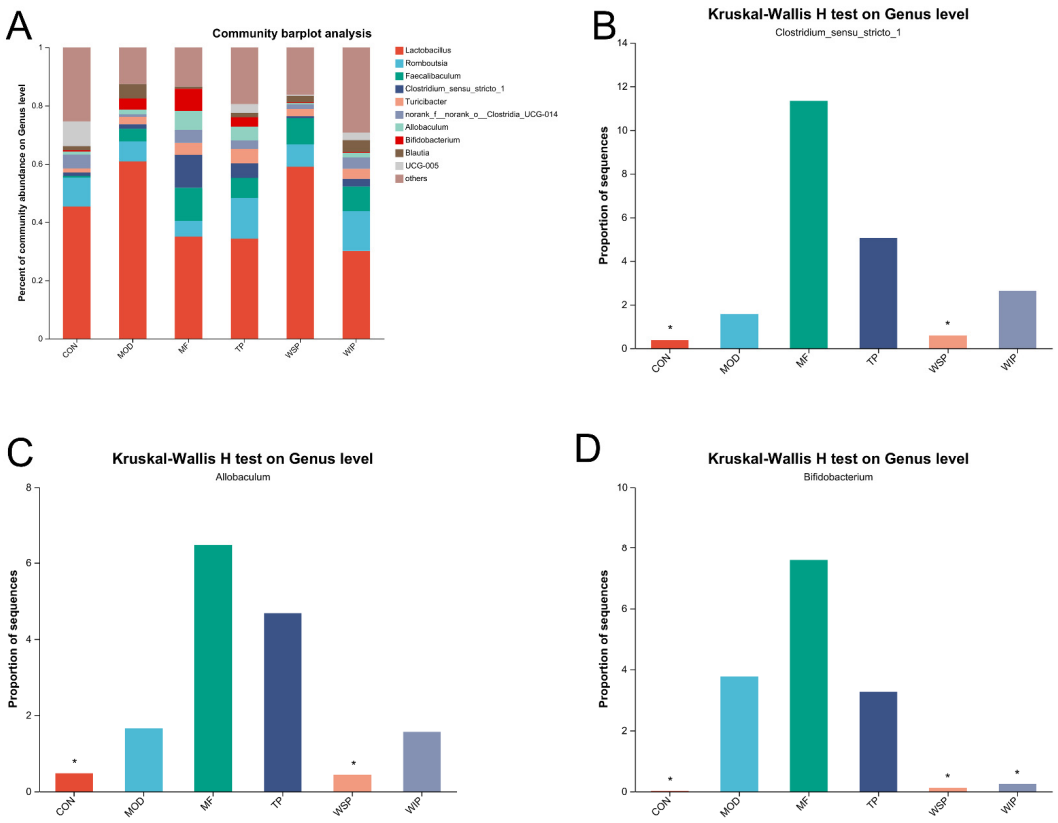

FIGURE 9. Effects of TP, WSP, and WIP on species composition and species difference of gut microbiotas in GLMD rats at the genus level. Sprague Dawley rats were treated with saline, MF (90 mg/kg/day), TP, WSP, or WIP (75, 150, or 300 mg/kg/day). The cecum content was collected after 10 weeks of HFHSD feeding for 16S rRNA sequencing analysis. Effects of TP, WSP, and WIP on species composition at the genus level (A). Effects of TP, WSP, and WIP on species difference of gut microbiota at the genus level (B-D). Results are expressed as mean ± S.D. from 3 animals. *$P < 0.05$, **$P < 0.01$, ***$P < 0.001$ *vs*. MOD group.

Fig. 10A shows the top ten most abundant species in the intestine of the rats treated with TP, WSP, and WIP, such as *s__Lactobacillus_murinus*, *s__Romboutsia_ilealis*, *s__Lactobacillus_reuteri*, *s__Lactobacillus_intestinalis*, *s__Lactobacillus_johnsonii*, *s__unclassified_f__Lachnospiraceae, s__uncultured_bacterium_g__Faecalibaculum*,

s__uncultured_bacterium_g__Clostridium_sensu_stricto_1, *s__unclassified_g__Lactobacillus*, and *s__uncultured_bacterium_g__Turicibacter*. The relative abundance of *s__uncultured_bacterium_g__Clostridium_sensu_stricto_1* significantly increased after 10 weeks of HFHSD feeding (Fig. 10B). However, the relative abundance of *s__uncultured_bacterium_g__Clostridium_sensu_stricto_1* significantly decreased after WSP treatment, while this significant change was not observed after the treatment with TP and WIP. These results showed that

WSP alleviated GLMD through the regulation of *s__uncultured_bacterium_g__Clostridium_sensu_stricto_1*, while TP and WIP did not have any significant regulatory effect on this gut microbiota.

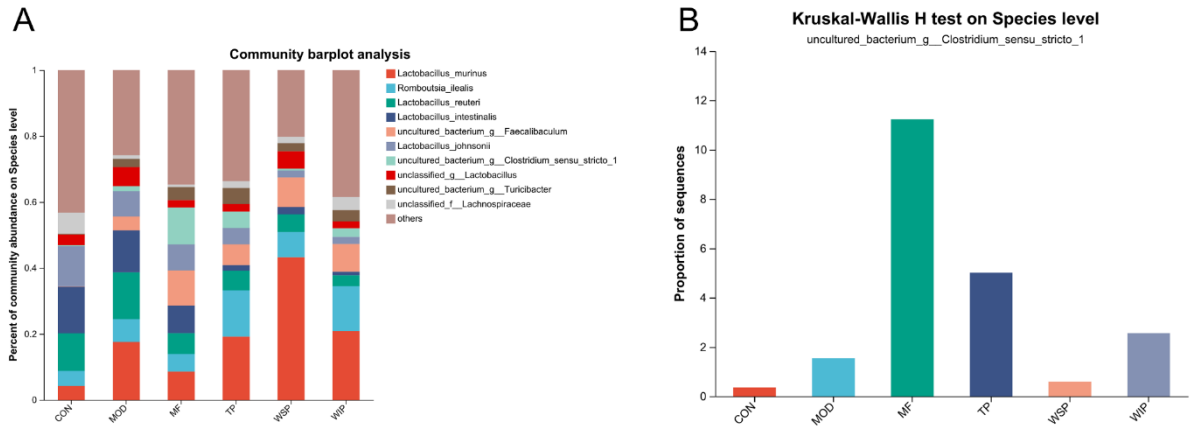

FIGURE 10. Effects of TP, WSP, and WIP on species composition and species difference of gut microbiotas in GLMD rats at the species level. Sprague Dawley rats were treated with saline, MF (90 mg/kg/day), TP, WSP, or WIP (75, 150, or 300 mg/kg/day). The cecum content was collected after 10 weeks of HFHSD feeding for 16S rRNA sequencing analysis. Effects of TP, WSP, and WIP on species composition at the species level (A). Effects of TP, WSP, and WIP on species difference of gut microbiota at the species level (B). Results are expressed as mean ± S.D. from 3 animals. *$P < 0.05$, **$P < 0.01$, ***$P < 0.001$ *vs*. MOD group.

3.6. Correlation analysis between the gut microbiotas, pharmacodynamic indexes and differential metabolites

3.6.1. Correlation between the gut microbiotas and pharmacodynamic indexes significantly regulated by WSP and WIP

Spearman correlation analysis was used to analyze the correlation between the top ten abundant gut microbiota and the relevant clinical indicators of drug efficacy at the phylum and genus level. At the phylum level, Actinobacteriota showed a positive correlation with liver TC, TG, and LDL-C, and a negative correlation with liver HDL-C and serum ACH (Fig. S7A). Bacteroidota showed a positive correlation with serum ACH, and a negative correlation with liver LDL-C. Spirochaetota showed a negative correlation with liver TC and TG. At the genus level, *Clostridium_sensu_stricto_1* and *Allobaculum* showed a positive correlation with liver TC, TG, and LDL-C, and a negative correlation with liver HDL-C and serum INS and ACH (Fig. S7B). *Bifidobacterium* showed a positive correlation with liver TG and LDL-C, and a negative correlation with serum ACH. These results showed that Actinobacteriota, Bacteroidota, Spirochaetota, *Clostridium_sensu_stricto_1*, *Allobaculum,* and *Bifidobacterium* were correlated with the efficacy indexes of drugs.

3.6.2. Correlation between the gut microbiotas and differential metabolites significantly regulated by WSP

At the phylum level, Actinobacteriota showed a negative correlation with serum diethylpropion, 2-nitrophenol and PC (2:0/PGD2), and a positive correlation with 4-oxo-L-proline, 9-octadecenamide, and 5-methyldeoxycytidine (Fig. S8A). Bacteroidota showed a negative correlation with serum metabolites such as 4-oxo-L-proline, gemfibrozil and artemisin, and a positive correlation with 1-nonanol, sphinganine, and arachidoyl ethanolamide. Moreover, Spirochaetota showed a negative correlation with serum methyl hexyl ether and 24-hydroxytetracosanoic acid.

At the genus level, *Clostridium_sensu_stricto_1* showed a negative correlation with serum C75 trans (Fig. S8B). *Allobaculum* showed a negative correlation with serum PC (2:0/PGD2) and propionylcarnitine, and a positive correlation with serum 9-octadecenamide and 4-hydroxy-2,6-dimethylaniline. Moreover, *Bifidobacterium* showed a positive correlation with serum lysoPC (18:3 (6Z, 9Z, 12Z)/0:0), isothankunic acid and zingerone.

At the phylum level, Actinobacteriota showed a negative correlation with urine metabolites such as L-phenylalanine, tyramine and L-tyrosine, and a positive correlation with metabolites such as D-glucuronic acid, 10-hydroxy-2E-decenoic acid and methylimidazoleacetic acid (Fig. S8C). Bacteroidota showed a negative correlation with urine metabolites such as dehydrooreadone, sulfinpyrazone and 2-aminopyrimidine, and a positive correlation with metabolites such as L-lysine, L-tyrosine and L-histidinol. Moreover, Spirochaetota showed a negative correlation with the urine metabolites such as kojic acid, apigenin-7-glucuronide and 1-nitro-7-hydroxy-8-glutathionyl-7,8-dihydronaphthalene, and a positive correlation with the metabolites such as acetyl-7-O-acetylneuraminic acid, L-lysine, and L-histidinol.

At the genus level, *Clostridium_sensu_stricto_1*, *Allobaculum,* and *Bifidobacterium* showed a negative correlation with the urine metabolites such as L-tyrosine, L-histidinol, L-lysine and sparfloxacin, and a positive correlation with the metabolites such as 2-aminopyrimidine, N-ethylguanidine, and 1,1-dimethylbiguanide (Fig. S8D).

At the phylum level, Actinobacteriota showed a negative correlation with liver resolvin E2 and epsilon-caprolactone, and a positive correlation with the metabolites such as (5E)-3-hydroxyhept-5-enoylcarnitine, citramalic acid and sphingosylphosphorylcholine (Fig. S8E). Bacteroidota showed a negative correlation with the liver metabolites such as (5E)-3-hydroxyhept-5-enoylcarnitine, citramalic acid and PC(16:0/PGF1alpha), and a positive correlation with the metabolites such as desacetyl-alacepril, resolvin E2 and 1-methyladenosine. Moreover, Spirochaetota showed a negative correlation with liver N-linoleoyl serine, and a positive correlation with desacetyl-alacepril.

At the genus level, *Clostridium_sensu_stricto_1* showed a negative correlation with liver 5'-deoxy-5-fluorocytidine and epsilon-caprolacton, and a positive correlation with the metabolites such as PE (18:4(6Z,9Z,12Z,15Z)/20:1(11Z)), (+/-)-(Z)-2-(5-tetradecenyl)cyclobutanone and sclareol oxide (Fig. S8F). *Allobaculum* showed a negative correlation with liver ergocornine and epsilon-caprolactone, and a positive correlation with the metabolites such as d-arabitol, citramalic acid, and (5E)-3-hydroxyhept-5-enoylcarnitine. Moreover, *Bifidobacterium* showed a negative correlation with liver 2-[(4-ethoxyphenyl) methylene]-3,4-dihydro-1(2H)-naphthalenone, and epsilon-caprolactone, and a positive correlation with the metabolites such as lysoPI (18:1 (9Z)/0:0), D-arabitol and citramalic acid.

Together, these results revealed that WSP alleviated GLMD through the regulation of the relative abundance of gut microbiota and the changes of related endogenous differential metabolites.

3.6.3. Correlation between the gut microbiotas and different metabolites significantly regulated by WIP

At the phylum level, Actinobacteriota showed a negative correlation with serum diethylpropion, 2-nitrophenol and nitrosobenzene, and a positive correlation with DL-p-chlorophenylalanine methyl ester hydrochloride, 5-methyldeoxycytidine and laurdan (Fig. S9A). Bacteroidota showed a negative correlation with the serum metabolites such as artemisin, gemfibrozil and cromakalim, and a positive correlation with the metabolites such as 4-hydroxysphinganine, lauryldiethanolamine and coumarin.

At the genus level, *Clostridium_sensu_stricto_1* showed a positive correlation with serum PC (18:0/20:4(8Z,11Z,14Z,17Z)) (Fig. S9B). *Allobaculum* showed a negative correlation with serum 4-hydroxysphinganine, and a positive correlation with serum PC (18:0/20:4(8Z, 11Z, 14Z, 17Z) and DG (20:5(5Z, 8Z, 11Z, 14Z, 16E)-OH (18R)/14:0/0:0). Moreover, *Bifidobacterium* showed a negative correlation with serum 4-hydroxysphinganine, and a positive correlation with PC (18:0/20:4 (8Z, 11Z, 14Z, 17Z).

At the phylum level, Actinobacteriota showed a negative correlation with the urine metabolites such as clofibric acid, indole-3-acetyl-tyrosine and PE (18:1(9Z)/0:0), and a positive correlation with the metabolites such as NNAL-N-glucuronide, (2S)-2-butanol O-(b-D-apiofuranosyl-(1- > 6)-b-D-glucopyranoside) and 5-keto-D-gluconate (Fig. S9C). Bacteroidota showed a negative correlation with the urine metabolites such as NNAL-N-glucuronide, (2S)-2-butanol O-(b-D-apiofuranosyl-(1- > 6)-b-D-glucopyranoside) and 4-hydroxyphenylacetic acid, and a positive correlation with the metabolites such as uralenneoside, isofebrifugine and CC12C(CC(CC1)C2(C)C)=CC(O)N. Moreover, Spirochaetota showed a negative correlation with the urine metabolites such as naringenin-7-O-beta-D-glucuronide and 1-nitro-7-hydroxy-8-glutathionyl-7,8-dihydronaphthalene, and a positive correlation with indole-3-acetyl-tyrosine and 4-amino-4-deoxyarabinose.

At the genus level, *Clostridium_sensu_stricto_1*, *Allobaculum* and *Bifidobacterium* showed a negative correlation with the urine metabolites such as phenytoin methylcatechol, 5-fluorouridine and 2-aminobutan-1-ol, and a positive correlation with the metabolites such as 1,1-dimethylbiguanide, metformin and NNAL-N-glucuronide (Fig. S9D).

At the phylum level, Actinobacteriota showed a positive correlation with the liver metabolites such as PC(18:1(9Z)/16:1(9Z)), muramic acid, and sphingosylphosphorylcholine (Fig. S9E). Bacteroidota showed a negative correlation with the liver metabolites such as 3-ureido-isobutyrate, ureidoisobutyric acid and melleolide, and a positive correlation with the metabolites such as isofebrifugine, dihydroroseoside and 2,8-quinolinediol. Moreover, Spirochaetota showed a positive correlation with liver 2,8-quinolinediol.

At the genus level, *Clostridium_sensu_stricto_1* showed a negative correlation with liver dihydroroseoside and 5'-deoxy-5-fluorocytidine, and a positive correlation with the metabolites such as GPEtn(18:3/18:1), PE(16:0/20:4(5Z,8Z,11Z,14Z)) and PC(16:0/18:1(11Z)) (Fig. S9F). *Allobaculum* showed a negative correlation with liver dihydroroseoside and ergocornine, and a positive correlation with the metabolites such as GPEtn(18:3/18:1), PE(16:0/20:4(5Z,8Z,11Z,14Z)) and PC(16:0/18:1(11Z)). Moreover, *Bifidobacterium* showed a negative correlation with liver dihydroroseoside, and a positive correlation with the metabolites such as PC(16:0/18:1(11Z)), lysoPI(18:0/0:0) and melleolide.

Together, these results revealed that WIP alleviated GLMD through the regulation of the relative abundance of gut microbiota and the changes of related endogenous differential metabolites.

3.6.4. Correlation among the gut microbiotas, metabolic pathways, differential metabolites, and pharmacodynamic indexes significantly regulated by WSP

WSP alleviated GLMD through the reduction of the relative abundance of Actinobacteriota to reduce the levels of TC, TG, and LDL-C in liver, and increased the level of HDL-C in the liver and ACH in serum, which might be related to the activation of tyrosine metabolism and the increase of tyrosine and L-tyrosine metabolites (Fig. S10A). WSP also alleviated GLMD through the increase of the relative abundance of Bacteroidota to reduce the level of LDL-C in the liver, and increased the level of ACH in the serum, which might be related to the activation of tyrosine, histidine, and sphingolipid metabolism, lysine degradation, and lysine biosynthesis, the increase of the metabolites L-tyrosine, 2-oxoadipic acid, 2-ketoglutaric acid, L-lysine, L-histidinol and sphinganine, and the decrease of p-coumaric acid and methylimidazoleic acid. Moreover, WSP alleviated GLMD through the increase of the abundance of Spirochaetota to reduce the levels of TC and TG in the liver, which might be related to the activation of histidine metabolism, lysine degradation, and lysine bioanabolic pathways and the up-regulation of L-lysine and L-histidinol.

WSP alleviated GLMD through the decrease of the relative abundance of *Clostridium_sensu_stricto_1* to activate tyrosine and histidine metabolism, lysine degradation, and lysine anabolic pathways, and increased the metabolites L-tyrosine, L-histidinol, tyramine, and L-lysin (Fig. S10B). WSP also alleviated GLMD through the decrease of the relative abundance of *Allobaculum* to activate tyrosine and histidinol metabolism pathways, and increased the metabolites L-tyrosine and L-histidinol. Moreover, WSP alleviated GLMD through the decrease of the relative abundance of *Bifidobacterium* to reduce the levels of TG and LDL-C in the liver, and increased the levels of ACH in the serum, which might be related to the activation of tyrosine and histidine metabolism, lysine degradation and lysine bioanabolic pathways, as well as the upregulation of the metabolites L-tyrosine, L-histidinol, tyramine, and L-lysine.

4. Discussion

With the change of life style, GLMD has emerged as a prominent chronic condition contributing to significant public health and clinical challenges on a global scale, posing a serious threat to human health. The liver is a key organ for glucose and lipid metabolism, responsible for maintaining stable blood glucose levels and promoting normal lipid metabolic processes. Our results showed that TP, WSP, and WIP improved the pathological status of the liver induced by HFHSD and reduced the deposition of lipid droplets. Furthermore, TP, WSP, and WIP alleviated lipid metabolic disorders in serum and liver by decreasing the levels of TC, TG, LDL-C, AST, and ALT, while increasing HDL-C levels. Additionally, TP, WSP, and WIP mitigated insulin resistance in GLMD rats by reducing FBG and INS levels. Thus, TP, WSP, and WIP alleviated GLMD by regulating glucose and lipid metabolism, and they constitute the main material basis for PC's efficacy against GLMD.

Prolonged consumption of HFHSD results in an exacerbation of inflammatory responses in the body and impairment of the gastrointestinal function, aggravating disturbances in glucose and lipid metabolism[29, 30].However, TP, WSP, and WIP inhibited the pathological injury on gastric and small intestinal tissues in GLMD rats. Furthermore, TP treatment induced a significant decrease in the levels of IL-6 and IL-1β and a significant increase in the levels of IL-2, ACH, and MTL in the serum. Notably, low TP doses were more effective compared to high TP doses, specifically the remedy for inflammation-related (IL-6) and gastrointestinal function-associated (ACH and MTL) biomarkers. This may be attributed to the complex composition of TP and the underlying pharmacological mechanisms (for example, the mode of action featuring multiple components, multiple pathways, and multiple targets), or the dosages used might not fall within the range of dose-response of TP. WSP treatment induced a significant decrease in the levels of IL-6 and IL-1β and a significant increase in the levels of IL-2 and ACH in the serum, while the levels of MTL, GAS and D-xylose in the urine showed an increasing trend. WIP treatment resulted in a significant decrease in the level of IL-6 and a significant increase in the levels of IL-2, ACH, MTL and GAS in the serum, while the level of D-xylose in the urine showed an increasing trend. This is consistent with the results reported in the literatures[29, 30]. Therefore, TP, WSP, and WIP improved the gastrointestinal function to relief GLMD.

When excessive glucose and lipids are absorbed into the bloodstream, their metabolism becomes challenging for the body, resulting in their storage in the liver, leading to hepatic damage and exacerbation of GLMD. This study revealed that the intervention with TP mitigated the ultrastructural damage of liver mitochondria. Furthermore, TP, WSP, and WIP increased the levels of MRCC II, Ca^{2+}-Mg^{2+}-ATPase, GSH, MRCC I, and Na^{+}-K^{+}-ATPase in liver mitochondria, while the level of MDA showed a decreasing trend. These findings suggested that TP, WSP, and WIP protected mitochondrial function by the mitigation of oxidative stress and the enhancement of energy metabolism, thus alleviating GLMD. Our previous study[29, 30] suggested that 15 active components of TP entered the liver mitochondria to treat non-alcoholic fatty liver disease, and these components may also be the main active substances of TP that regulate liver mitochondria to relieve GLMD. WSP and WIP enter the gastrointestinal tract and may not be directly absorbed into the liver mitochondria, but they may be decomposed into oligosaccharides or monosaccharides by intestinal flora and absorbed into liver mitochondria to remedy mitochondrial function. Additionally, they may also enter the gastrointestinal tract to regulate intestinal flora and then indirectly act on liver mitochondria.

This study used metabolomics to examine the effects of TP, WSP, and WIP on differential metabolites and metabolic pathways in the serum, urine, and liver. The metabolites returned to the normal level after the administration of TP, WSP, and WIP. TP regulated 588 different metabolites, which were mainly involved in lipid, amino acid, cofactor, and vitamin metabolism, as well as xenobiotic biodegradation and metabolism. WSP regulated 500 distinct metabolites, which were mainly involved in lipid, amino acid, cofactor, and vitamin metabolism. WIP regulated 308 endogenous metabolites, which were mainly involved in the metabolism of lipids, amino acids and biosynthesis of other secondary metabolites. LCAT, LPCAT2 and EPT1 are the key enzymes involved in regulating the decomposition or synthesis of lecithin and

phosphatidylethanolamine in the metabolism of glycerophospholipid. sPLA2 is a key enzyme in arachidonic acid metabolism, which promotes the decomposition of lecithin and synthesis of arachidonate. ALDH7A1 is a key enzyme that promotes the synthesis of L-2-aminoadipate in lysine degradation. Changes in metabolites may be attributed to the regulation of key enzymes by TP, WSP, and WIP, such as LCAT, LPCAT2, EPT1, sPLA2, and ALDH7A1. LCAT improves lipid metabolism disorder by promoting formation of high density lipoprotein cholesterol, enhancing cholesterol reverse transport[31]. Defects in LCAT may increase the risk of insulin resistance[32]. ALDH7A1 catalyzes lipoaldehyde detoxification and α-aminoadipic acid metabolism, protects beta cells from oxidative damage and can be used as a biomarker to predict type 2 diabetes risk[33]. EPT1 catalyzes phosphatidylethanolamine synthesis, and the deficiency of EPT1 leads to the reduction of phosphatidylethanolamine, impacts insulin receptor membrane localization and signaling, and inhibits β-oxidation and energy metabolism[34]. The increase of sPLA2 level aggravates atherosclerosis and insulin resistance, which is closely related to glucose and lipid metabolism[35]. LPCAT2 catalyzes phospholipid remodeling, affecting membrane lipid composition and inflammatory signals. It promots the production of pro-inflammatory lipids, aggravats obesity-related inflammation and insulin resistance, and is up-regulated in the liver of patients with nonalcoholic fatty liver disease, promoting the accumulation of triglycerides[36-38]. TP increased the levels of LPCAT2, LCAT, and EPT1, downregulated the level of sPLA2, and upregulated the level of ALDH7A1. WSP increased the levels of EPT1, LCAT and ALDH7A1. WIP increased the levels of EPT1, LPCAT2, LCAT, and ALDH7A1. These results suggested that TP, WSP, and WIP mainly regulated lipid, amino acid, cofactor, and vitamin metabolism to improve GLMD. Notably, TP and WIP administration significantly elevated LPCAT2 levels, consistent with prior observations of increased LPCAT2 expression in on-alcoholic fatty liver disease and non-alcoholic steatohepatitis[38]. Whether the increase of LPCAT2 level is conducive to GMD treatment needs in-depth research.

Gut microbiota is critical to human health and is closely associated with many chronic diseases such as GLMD. Polysaccharides and triterpenes can reach the large intestine without being digested, demonstrating the potential of probiotics to be involved in the regulation GLMD and maintenance of human health[13, 39]. The alpha diversity analysis revealed that TP, WSP, and WIP increased the richness and diversity of gut microbiome. The community structure of the gut microbiome was closer to the normal status after the treatment with TP, WSP, and WIP, which induced a significant reorganization of the gut microbiome at the phylum, genus, and species levels. WSP decreased the relative abundance of Actinobacteriota, *Clostridium_sensu_stricto_1*, *Allobaculum*, *Bifidobacterium*, and the *uncultured bacterium g_Clostridium_sensu_stricto_1*, while increased the relative abundance of Spirochaetota and Bacteroidota. WIP reduced the relative abundance of Actinobacteriota and *Bifidobacterium*. However, TP did not significantly regulate the gut microbiome at the phylum, genus, and species levels. These results indicated that WSP and WIP regulated the relative abundance of gut microbiota, thereby alleviating GLMD.

At the phylum level, Actinobacteriota showed a significant positive correlation with TC, TG, and LDL-C in the liver, and a significant negative correlation with HDL-C and ACH in the serum. Bacteroidota showed a

significant negative correlation with LDL-C in the liver and a significant positive correlation with ACH in the serum. Additionally, Spirochaetota was significantly negatively correlated with TC and TG levels in the liver. These results indicated that Actinobacteriota, Bacteroidota, and Spirochaetota in the gut microbiota were significantly regulated by WSP or WIP, and associated with pharmacological indicators related to GLMD. Previous studies reported that an increase in Actinobacteriota is a common marker of obesity, and the expression of Cebpa (a key enzyme involved in fat synthesis) in rat liver is positively correlated with Actinobacteriota[40]. Furthermore, existing literature indicates that a reduction in *Actinobacteria* is advantageous for the management of diabetes, obesity, hyperlipidemia, and other carbohydrate-dependent diseases[41]. Bacteroidota constitutes a crucial microbial community involved in maintaining intestinal microbial homeostasis in the body. Alterations in Bacteroidota lead to changes in its metabolic functions, including nutrient digestion and energy absorption, potentially resulting in inflammatory diseases such as obesity, diabetes, atherosclerosis, and neurodegenerative disorders[42]. Bacteroidota was negatively correlated with obesity[43]. Furthermore, members of the *Bacteroides* synthesize conjugated linoleic acid and possess anti-diabetes, anti-atherosclerosis, anti-obesity, lipid-lowering, and immune-modulating properties[44]. This study revealed that the relative abundance of Spirochaetota was significantly increased after the administration of WSP, which might represent a potential mechanism underlying its effects on mitigating GLMDs. However, no literature is currently available documenting its association with GLMD, indicating that further research is needed.

At the genus level, *Clostridium sensu stricto 1* and *Allobaculum* showed a positive correlation with TC, TG, and LDL-C in the liver, and a negative correlation with HDL-C, as well as INS and ACH in the serum. *Bifidobacterium* showed a positive correlation with TG and LDL-C in the liver, and a negative correlation with ACH in the serum. These findings indicated that *Clostridium sensu stricto 1*, *Allobaculum*, and *Bifidobacterium* that were significantly regulated by WSP or WIP were associated with pharmacological indexs related to GLMD. Furthermore, *Clostridium sensu stricto 1* influences metabolic health by affecting type 1 diabetes, inflammation, inflammatory bowel disease, type 2 diabetes, and obesity[45-48]. *Clostridium sensu stricto 1* in obese patients with metabolic abnormalities shows a positive correlation with body weight and blood lipid (LDL-C, TC and TG), and it is a biomarker for obesity-related metabolic disorders[49]. *Erysipelotrichia* is associated with liver steatosis, and *Allobaculum*, a member of the *Erysipelotrichia*, produces short-chain fatty acids, and these short-chain fatty acids produced by intestinal microorganisms are an additional source of energy for humans and directly or indirectly affect non-alcoholic fatty liver disease[50]. *Allobaculum* was negatively correlated with obesity[43]. Existing literature indicates that *Allobaculum* is positively correlated with diabetes and diabetic nephropathy[51]. Additionally, the low abundance of *Bifidobacterium* is a marker for the intestinal microbiome in type 2 diabetes and contributes to the acceleration of its progression[52]. *Bifidobacterium* mitigates GLMD induced by obesity and high fat diet through the production of succinic acid and secondary bile acids[36]. The existing literature predominantly supports the notion that an increase in the relative abundance of *Bifidobacterium* is advantageous in the regulation of

GLMD. Nevertheless, our results revealed that the relative abundance of *Bifidobacterium* significantly decreased after WSP and WIP treatment, which deserves a thorough investigation.

The relationship between differential metabolites and gut microbiota significantly regulated by WSP revealed that, at the phylum level, Actinobacteriota was negatively correlated with the metabolites such as PC (2:0/PGD2), tyramine, L-tyrosine, epsilon-caprolactone, and positively correlated with the metabolites such as 4-oxo-L-proline, methylimidazoleacetic acid, and sphingosylphosphorylcholine. Bacteroidota was negatively correlated with the metabolites such as P-coumaric acid, methylimidazoleacetic acid, and PC (16:0/PGF1alpha), and positively correlated with the metabolites such as L-lysine, L-histidinol, and sphinganine. Spirochaetota was negatively correlated with the metabolites such as 24-hydroxytetracosanoic acid, N-linoleoyl serine, and kojic acid, and positively correlated with the metabolites such as desacetyl-alacepril, L-lysine, and L-histidinol. At the genus level, *Clostridium_sensu_stricto_1* was negatively correlated with the metabolites such as C75 trans, L-tyrosine, L-histidinol, tyramine, and L-lysine, and positively correlated with the metabolites such as PE(18:4(6Z,9Z,12Z,15Z)/20:1(11Z)) and 2-aminopyrimidine. *Allobaculum* was negatively correlated with the metabolites such as PC(2:0/PGD2), L-tyrosine, epsilon-caprolactone, and (5E)-3-hydroxyhept-5-enoylcarnitine, and positively correlated with the metabolites such as 9-octadecenamide and 2-aminopyrimidine. *Bifidobacterium* was negatively correlated with the metabolites such as L-tyrosine, L-histidinol, tyramine, and L-lysine, and positively correlated with the metabolites such as LysoPI(18:1(9Z)/0:0) and 2-aminopyrimidine.

Similarly, the relationship between differential metabolites and gut microbiota significantly regulated by WIP revealed that, at the phylum level, Actinobacteriota was negatively correlated with the metabolites such as diethylpropion, clofibric acid, and PE (18:1(9Z)/0:0), and positively correlated with the metabolites such as 5-methyldeoxycytidine, NNAL-N-glucuronide, and sphingosylphosphorylcholine. At the genus level, *Bifidobacterium* was negatively correlated with the metabolites such as 4-hydroxysphinganine, phenytoin methylcatechol, and dihydroroseoside, and positively correlated with the metabolites such as 1,1-dimethylbiguanide, PC (18:0/20:4(8Z,11Z,14Z,17Z), and PC(16:0/18:1(11Z)). Consequently, WSP and WIP regulated the abundance of intestinal microbiota and thus rearranged the endogenous metabolites in the serum, urine, and liver to normal levels, which represented a potential mechanism in the treatment of GLMD.

The analysis of the correlation among intestinal flora, metabolic pathways, differential metabolites and pharmacodynamic indicators revealed that WSP significantly regulated the relative abundance of Actinobacteriota, Spirochaetota, Bacteroidota, *Clostridium_sensu_stricto_1*, *Allobaculum*, and *Bifidobacterium* at the phylum or genus level, thereby activating different metabolic pathways such as tyrosine, histidine, and sphingolipid metabolism, lysine degradation, and lysine biosynthesis, affecting the levels of metabolites such as L-tyrosine, L-histidinol, tyramine, L-lysine, 2-oxoadipic acid, 2-ketoglutaric acid, and sphinganine to improve TC, TG, LDL-C, HDL-C, and ACH levels, ultimately ameliorating GLMD. WIP and TP were not able to create a relationship among the gut microbiome, pharmacodynamic markers, and differential metabolites.

5. Conclusion

TP, WSP, and WIP alleviated HFHSD-induced GLMD by improving gastrointestinal and liver mitochondrial function. TP regulated lipid, amino acid, cofactor, and vitamin metabolism and xenobiotic biodegradation and metabolism. WSP regulated lipid, amino acid, cofactor, and vitamin metabolism. WIP regulated lipid, amino acid and the biosynthesis of other secondary metabolites. TP, WSP, and WIP also regulated the diversity, richness, and community structure of gut microbiome to against GLMD. WSP decreased the relative abundance of Actinobacteriota, *Clostridium_sensu_stricto_1*, *Allobaculum*, *Bifidobacterium*, and the *uncultured bacterium g_Clostridium_sensu_stricto_1*, while increased the relative abundance of Spirochaetota and Bacteroidota. WIP reduced the relative abundance of Actinobacteriota and *Bifidobacterium*. TP, WSP, and WIP constitute the main material basis for PC's efficacy against GLMD.

Acknowledgments

Not applicable.

Availability of data and materials

All the data supporting the findings of this study are available from the corresponding author upon request.

Competing interests

The authors declare that there is no duality of interest associated with the publication of this manuscript.

Consent for publication

All the authors have approved the manuscript for publication.

References

[1] R.H. Eckel, S.M. Grundy, P.Z. Zimmet, The metabolic syndrome, Lancet. 365 (2005) 1415-1428. https://doi.org/10.1016/s0140-6736(05)66378-7.

[2] P.Z. Zimmet, D.J. Magliano, W.H. Herman, et al., Diabetes: a 21st century challenge, Lancet Diabetes Endocrinol. 2 (2014) 56-64. https://doi.org/10.1016/s2213-8587(13)70112-8.

[3] R. Liu, F. Zhang, X. He, et al., Plant Derived Exosome-Like Nanoparticles and Their Therapeutic Applications in Glucolipid Metabolism Diseases, J Agric Food Chem. 73 (2025) 6385-6399. https://doi.org/10.1021/acs.jafc.4c12480.

[4] P. Xiong, F. Zhang, F. Liu, et al., Metaflammation in glucolipid metabolic disorders: Pathogenesis and treatment, Biomed. Pharmacother. 161 (2023) 114545. https://doi.org/10.1016/j.biopha.2023.114545.

[5] N. Owen, G.N. Healy, C.E. Matthews, et al., Too much sitting: the population health science of sedentary behavior, Exerc. Sport Sci. Rev. 38 (2010) 105-113. https://doi.org/10.1097/JES.0b013e3181e373a2.

[6] M.T. Hamilton, D.G. Hamilton, T.W. Zderic, Role of low energy expenditure and sitting in obesity, metabolic syndrome, type 2 diabetes, and cardiovascular disease, Diabetes. 56 (2007) 2655-2667. https://doi.org/10.2337/db07-0882.

[7] L. Zhu, C. Ye, B. Hu, et al., Regulation of gut microbiota and intestinal metabolites by *Poria cocos* oligosaccharides improves glycolipid metabolism disturbance in high-fat diet-fed mice, J. Nutr. Biochem. 107 (2022) 109019. https://doi.org/10.1016/j.jnutbio.2022.109019.

[8] Y. Duan, J. Huang, M. Sun, et al., *Poria cocos* polysaccharide improves intestinal barrier function and maintains intestinal homeostasis in mice, Int. J. Biol. Macromol. 249 (2023) 125953. https://doi.org/10.1016/j.ijbiomac.2023.125953.

[9] Z. Wang, Y. Shi, X. Zhang, et al., Research progress in the ethnopharmacology, phytochemistry, pharmacology, toxicology, and quality control of *Valeriana jatamansi* Jones, J. Ethnopharmacol. 332 (2024) 118403. https://doi.org/10.1016/j.jep.2024.118403.

[10] C.W.Zhang, Z. Yu, S. Shan, et al., Research progress on herbalism, chemical constituents and pharmacological effects of different medicinal parts of *Poria cocos*, Hubei Agric. Sci. 60 (2021) 9-14+19. https://doi.org/10.14088/j.cnki.issn0439-8114.2021.02.002.

[11] J. Zuo, T.L. Qi, X.Y. Hu, Research Progress in Chemical Constituents and Modern Pharmacology of *Poria Cocos*, Acta Chin. Med. Pharmacol. 51 (2023) 110-114. https://doi.org/10.19664/j.cnki.1002-2392.230022.

[12] Y. Yang, X.L. Huang, Z.M. Jiang, et al., Quantification of Chemical Groups and Quantitative HPLC Fingerprint of *Poria cocos* (Schw.) Wolf, Molecules. 27 (2022) 6383 https://doi.org/10.3390/molecules27196383.

[13] Y.-K. Xie, X.-Y. Pan, X.-R. Liang, et al., Research progress on structural characterization and bioactivities of *Poria cocos* and Ganoderma polysaccharides, Food Med. Homol. 2 (2025) 9420040. https://doi.org/10.26599/FMH.2025.9420040.

[14] H. Wang, S. Shi, S. Wang, Can highly cited herbs in ancient Traditional Chinese medicine formulas and modern publications predict therapeutic targets for diabetes mellitus?, J. Ethnopharmacol. 213 (2018) 101-110. https://doi.org/10.1016/j.jep.2017.10.032.

[15] S.S. Sun, K. Wang, K. Ma, et al., An insoluble polysaccharide from the sclerotium of *Poria cocos* improves hyperglycemia, hyperlipidemia and hepatic steatosis in ob/ob mice via modulation of gut microbiota, Chin. J. Nat. Med. 17 (2019) 3-14. https://doi.org/10.1016/s1875-5364(19)30003-2.

[16] Y.C. Huang, W.L. Chang, S.F. Huang, et al., Pachymic acid stimulates glucose uptake through enhanced GLUT4 expression and translocation, Eur. J. Pharmacol. 648 (2010) 39-49. https://doi.org/10.1016/j.ejphar.2010.08.021.

[17] C.H. Lin, Y.H. Kuo, C.C. Shih, Eburicoic Acid, a Triterpenoid Compound from *Antrodia camphorata*, Displays Antidiabetic and Antihyperlipidemic Effects in Palmitate-Treated C2C12 Myotubes and in High-Fat Diet-Fed Mice, Int. J. Mol. Sci. 18 (2017) 2314 https://doi.org/10.3390/ijms18112314.

[18] M. Sato, T. Tai, Y. Nunoura, et al., Dehydrotrametenolic acid induces preadipocyte differentiation and sensitizes animal models of noninsulin-dependent diabetes mellitus to insulin, Biol. Pharm. Bull. 25 (2002) 81-86. https://doi.org/10.1248/bpb.25.81.

[19] J. He, Y. Yang, F. Zhang, et al., Effects of *Poria cocos* extract on metabolic dysfunction-associated fatty liver disease via the FXR/PPARα-SREBPs pathway, Front. Pharmacol. 13 (2022) 1007274. https://doi.org/10.3389/fphar.2022.1007274.

[20] Y. Li, P. Wang, H. Yang, et al., In vivo identification of bioactive components of *Poria cocos* for adjusting mitochondria against metabolic dysfunction-associated fatty liver disease, Heliyon. 10 (2024) e35645. https://doi.org/10.1016/j.heliyon.2024.e35645.

[21] Y.Q. Yang, F.Y. Meng, X. Liu, et al., Distinct metabonomic signatures of Polygoni Multiflori Radix Praeparata against glucolipid metabolic disorders, J. Pharm. Pharmacol. 73 (2021) 796-807. https://doi.org/10.1093/jpp/rgab012.

[22] C.J. Lynch, S.H. Adams, Branched-chain amino acids in metabolic signalling and insulin resistance, Nat. Rev. Endocrinol. 10 (2014) 723-736. https://doi.org/10.1038/nrendo.2014.171.

[23] C. Ma, M. Han, B. Heinrich, et al., Gut microbiome-mediated bile acid metabolism regulates liver cancer via NKT cells, Science. 360 (2018) 5931 https://doi.org/10.1126/science.aan5931.

[24] S. Yang, R. Liu, Z. Xin, et al., Plasma Metabolomics Identifies Key Metabolites and Improves Prediction of Diabetic Retinopathy: Development and Validation across Multinational Cohorts, Ophthalmology. 131 (2024) 1436-1446. https://doi.org/10.1016/j.ophtha.2024.07.004.

[25] M. Thiele, I.F. Villesen, L. Niu, et al., Opportunities and barriers in omics-based biomarker discovery for steatotic liver diseases, J. Hepatol. 81 (2024) 345-359. https://doi.org/10.1016/j.jhep.2024.03.035.

[26] W.M. de Vos, H. Tilg, M. Van Hul, et al., Gut microbiome and health: mechanistic insights, Gut. 71 (2022) 1020-1032. https://doi.org/10.1136/gutjnl-2021-326789.

[27] W. Li, J. Yu, J. Zhao, et al., *Poria cocos* polysaccharides reduces high-fat diet-induced arteriosclerosis in ApoE(-/-) mice by inhibiting inflammation, Phytother. Res. 35 (2021) 2220-2229. https://doi.org/10.1002/ptr.6980.

[28] X.X. Yang, F. Xu, D. Wang, et al., Development of a mitochondria-based centrifugal ultrafiltration/liquid chromatography/mass spectrometry method for screening mitochondria-targeted bioactive constituents from complex matrixes: Herbal medicines as a case study, J. Chromatogr. A. 1413 (2015) 33-46. https://doi.org/10.1016/j.chroma.2015.08.014.

[29] L. Conterno, F. Fava, R. Viola, et al., Obesity and the gut microbiota: does up-regulating colonic fermentation protect against obesity and metabolic disease?, Genes Nutr. 6 (2011) 241-260. https://doi.org/10.1007/s12263-011-0230-1.

[30] P.V. Ocampo-Anguiano, L.L. Victoria-Ruiz, R. Reynoso-Camacho, et al., Ingestion of Bean Leaves Reduces Metabolic Complications and Restores Intestinal Integrity in C57BL/6 Mice with Obesity Induced by a High-Fat and High-Fructose Diet, Nutrients. 16 (2024) 367 https://doi.org/10.3390/nu16030367.

[31] A. Niemelä, L. Giorgi, S. Nouri, et al., Gliflozins, sucrose and flavonoids are allosteric activators of lecithin-cholesterol acyltransferase, Sci Rep. 14 (2024) 26085. https://doi.org/10.1038/s41598-024-77104-3.

[32] E. Xepapadaki, G. Maulucci, C. Constantinou, et al., Impact of apolipoprotein A1- or lecithin:cholesterol acyltransferase-deficiency on white adipose tissue metabolic activity and glucose homeostasis in mice, Biochim. Biophys. Acta Mol. Basis Dis. 1865 (2019) 1351-1360. https://doi.org/10.1016/j.bbadis.2019.02.003.

[33] C. Brocker, M. Cantore, P. Failli, et al., Aldehyde dehydrogenase 7A1 (ALDH7A1) attenuates reactive aldehyde and oxidative stress induced cytotoxicity, Chem. Biol. Interact. 191 (2011) 269-277. https://doi.org/10.1016/j.cbi.2011.02.016.

[34] Y. Chen, H. Jiang, Z. Zhan, et al., Restoration of lipid homeostasis between TG and PE by the LXRα-ATGL/EPT1 axis ameliorates hepatosteatosis, Cell Death Dis. 14 (2023) 85. https://doi.org/10.1038/s41419-023-05613-6.

[35] S.A. Khan, M.A. Ilies, The Phospholipase A2 Superfamily: Structure, Isozymes, Catalysis, Physiologic and Pathologic Roles, Int. J. Mol. Sci. 24 (2023) 1353 https://doi.org/10.3390/ijms24021353.

[36] W. Abate, H. Alrammah, M. Kiernan, et al., Lysophosphatidylcholine acyltransferase 2 (LPCAT2) co-localises with TLR4 and regulates macrophage inflammatory gene expression in response to LPS, Sci Rep. 10 (2020) 10355. https://doi.org/10.1038/s41598-020-67000-x.

[37] Z. Hall, N.J. Bond, T. Ashmore, et al., Lipid zonation and phospholipid remodeling in nonalcoholic fatty liver disease, Hepatology. 65 (2017) 1165-1180. https://doi.org/10.1002/hep.28953.

[38] M. Nam, M.S. Choi, J.Y. Choi, et al., Effect of green tea on hepatic lipid metabolism in mice fed a high-fat diet, J. Nutr. Biochem. 51 (2018) 1-7. https://doi.org/10.1016/j.jnutbio.2017.09.002.

[39] J.C. Kim, J.Y. Jeon, W.S. Yang, et al., Combined Amelioration of Ginsenoside (Rg1, Rb1, and Rg3)-enriched Korean Red Ginseng and Probiotic Lactobacillus on Non-alcoholic Fatty Liver Disease, Curr Pharm Biotechnol. 20 (2019) 222-231. https://doi.org/10.2174/1389201020666190311143554.

[40] M. Juárez-Fernández, D. Porras, P. Petrov, et al., The Synbiotic Combination of Akkermansia muciniphila and Quercetin Ameliorates Early Obesity and NAFLD through Gut Microbiota Reshaping and Bile Acid Metabolism Modulation, Antioxidants (Basel). 10 (2021) 2001 https://doi.org/10.3390/antiox10122001.

[41] Y. Xie, Z. Li, Y. Fan, et al., Integrated gut microbiome and UHPLC-MS metabolomics to reveal the prevention mechanism of pidanjiangtang granules on IGT Rats, Phytomedicine. 135 (2024) 156201. https://doi.org/10.1016/j.phymed.2024.156201.

[42] S. Liye, P. Yongming, X. Yanyun, et al., Changes in intestinal flora in a Wuzhishan minipig atherosclerosis model induced by high-fat and high-sugar diet, Acta Lab. Anim. Sci. Sin. 30 (2022) 299-308. https://link.cnki.net/urlid/11.2986.Q.20220607.1814.008

[43] Y.-M. Liu, C. Liu, Y.-S. Deng, et al., Beneficial effects of dietary herbs on high-fat diet-induced obesity linking with modulation of gut microbiota, Food & Med. Homol. 2 (2025) 9420034. https://doi.org/10.26599/FMH.2025.9420034.

[44] A.S. Wilson, K.R. Koller, M.C. Ramaboli, et al., Diet and the Human Gut Microbiome: An International Review, Dig Dis Sci. 65 (2020) 723-740. https://doi.org/10.1007/s10620-020-06112-w.

[45] H. Gao, Q. Jiang, H. Ji, et al., Type 1 diabetes induces cognitive dysfunction in rats associated with alterations of the gut microbiome and metabolomes in serum and hippocampus, Biochim. Biophys. Acta Mol. Basis Dis. 1865 (2019) 165541. https://doi.org/10.1016/j.bbadis.2019.165541.

[46] J. Xu, X. Chen, S. Yu, et al., Effects of Early Intervention with Sodium Butyrate on Gut Microbiota and the Expression of Inflammatory Cytokines in Neonatal Piglets, PLoS One. 11 (2016) e0162461. https://doi.org/10.1371/journal.pone.0162461.

[47] C.J. Kiely, P. Pavli, C.L. O'Brien, The microbiome of translocated bacterial populations in patients with and without inflammatory bowel disease, Intern Med J. 48 (2018) 1346-1354. https://doi.org/10.1111/imj.13998.

[48] Z. Qin, Z. Zhongkai, R. Xiaochong, et al., Comparision of Faecal Microbiota in Rats with Type 2 Diabetes and Non-Diabetic Rats Using Miseq High-throughput Sequencing, J. Chin. Inst. Food Sci. Technol. 17 (2017) 232-239. https://doi.org/10.16429/j.1009-7848.2017.06.031.

[49] Q. Zeng, D. Li, Y. He, et al., Discrepant gut microbiota markers for the classification of obesity-related metabolic abnormalities, Sci Rep. 9 (2019) 13424. https://doi.org/10.1038/s41598-019-49462-w.

[50] Y. Jung, I. Kim, M. Mannaa, et al., Effect of Kombucha on gut-microbiota in mouse having non-alcoholic fatty liver disease, Food Sci. Biotechnol. 28 (2019) 261-267. https://doi.org/10.1007/s10068-018-0433-y.

[51] B. Yao, B. Pan, T. Tian, et al., Baihu renshen decoction ameliorates type 2 diabetes mellitus in rats through affecting gut microbiota enhancing gut permeability and inhibiting TLR4/NF-κB-mediated inflammatory response, Front Cell Infect Microbiol. 12 (2022) 1051962. https://doi.org/10.3389/fcimb.2022.1051962.

[52] T. Jiang, Y. Li, L. Li, et al., Bifidobacterium longum 070103 Fermented Milk Improve Glucose and Lipid Metabolism Disorders by Regulating Gut Microbiota in Mice, Nutrients. 14 (2022) https://doi.org/10.3390/nu14194050.